3 Electrochemical characterization and mathematical modeling of zinc passivation in alkaline solutions: A review

Electrochimica Acta 237 (2017) 276–298

Contents lists available at ScienceDirect

Electrochimica Acta

journal homepage: www.elsevier.com/locate/electacta

Electrochemical characterization and mathematical modeling of zinc passivation in alkaline solutions: A review

Marina Bockelmann[a,b], Laurens Reining[a,b], Ulrich Kunz[a,b], Thomas Turek[a,b,*]

[a] Institute of Chemical and Electrochemical Process Engineering, Clausthal University of Technology, Clausthal-Zellerfeld 38678, Germany
[b] Energie-Forschungszentrum Niedersachsen, Am Stollen 19A, Goslar 38640, Germany

ARTICLE INFO

Article history:
Received 28 July 2016
Received in revised form 22 December 2016
Accepted 19 March 2017
Available online 21 March 2017

Keywords:
Zinc anodes
Passivation
Alkaline electrolyte
Mathematical modeling

ABSTRACT

Passivation of zinc electrodes caused by formation of oxy-products with low electrical conductivity is one of the most important phenomena which limits the current density during discharge and contributes to the poor cyclability of zinc-based batteries. The present review critically discusses the existing experimental findings related to passivation of zinc in alkaline electrolyte as well as the state of the mathematical modelling of this process. Despite numerous investigations over several decades, no general consensus about the underlying mechanisms and the strategies to prevent passivation could be achieved. Main reason for this uncertainty is that different processes can lead to passivation. On the one hand, precipitation of so-called type 1 films occurs above a critical zincate concentration while on the other hand the direct oxidation of the zinc surface takes place below a certain potential, leading to type 2 passive films. As long as formed films remain porous, passivation does not necessarily lead to complete breakdown of the electrode activity. It is therefore recommended to conduct further measurements employing a combination of techniques in which both the potential and the concentration of zincates at the electrode surface can be precisely controlled. It is also proposed to carry out systematic studies on the influence of temperature, electrolyte flow, and electrolyte composition – including additives – on the passivation time and the structure of the passive film. Finally, the purity and the structure of the zinc electrode may also have an influence on the passivation processes and should be considered during future studies.

1. Introduction

In 1796 Volta developed the first electrical primary battery with zinc as the anode material, which is today known as voltaic cell. Until now most batteries contain zinc as the negative electrode [1]. Zinc is considered a promising material for low-cost energy storage due to a number of decisive advantages. It has a low equilibrium potential and the highest energy density among those metals which can be reduced in aqueous electrolytes [2]. Furthermore, it is inexpensive, abundant [3] and has a low hazard potential. Based on these characteristics the next desirable step for further development of zinc-based systems would be the technical realization of electrically rechargeable zinc-air energy storage systems for stationary and mobile applications.

Discharging tests of zinc-based batteries show that the maximum usable capacity strongly depends on the current density and the operating conditions [4]. One of the most discussed causes for this effect is the occurring passivation of zinc anodes during the discharging process of the battery [5–7]. Passivation is enhanced at higher current densities so that zinc-based batteries are commonly applied in smaller electric devices at lower current level [4,8]. Due to the importance of zinc anodes for the development of batteries with high energy density, passivation studies of zinc electrodes in alkaline solutions should be one important focus of future battery research. It is generally accepted that after a period of active zinc dissolution the electrode becomes passive, caused by a layer of oxy-products covering the surface. It is necessary to understand the mechanism of passivation in order to choose appropriate operating conditions for increasing the utilization of zinc and the service life of the battery.

Since the beginning of the 19th century scientists have investigated the phenomenon of the passiveness of metals [9–14]. Schönbein discovered that a piece of iron in contact with diluted nitric acid dissolves and produces hydrogen, but if the iron

* Corresponding author at: Institute of Chemical and Electrochemical Process Engineering, Clausthal University of Technology, Clausthal-Zellerfeld, 38678, Germany.
E-mail address: turek@icvt.tu-clausthal.de (T. Turek).

http://dx.doi.org/10.1016/j.electacta.2017.03.143
0013-4686/

is placed in concentrated nitric acid and then returned to the dilute nitric acid, no reaction will take place. He described the changed state of iron as passive [9]. Vetter summarized in 1961 the achieved state of knowledge concerning the formation and the growth of a passive layer on metals [15]. In the active state, provided that the potential is sufficiently positive, metals dissolve directly according to the reaction $Me \rightarrow Me^{z+} + ze^{-}$. However, in strong oxidizing electrolytes or at too high anodic current densities a passive film can form directly on the electrode surface and prevent it from further dissolution.

The influence of the passive film on the performance of the metal electrode can be explained on the basis of its potential-current characteristics (Fig. 1). At potentials higher than the so-called Flade potential E_F a protective oxide film forms on the electrode and causes a considerable decrease of the current density [15]. Wagner proposed to define this current density drop as a criterion for electrode passivation [15]. However, not every passive film formation can be detected as a sharp decrease of the current density, thus a universal criterion for the passivation of a metal electrode still needs to be formulated. Furthermore, Vetter introduced the corrosion current density j_K (Fig. 1), which can be measured at potentials higher than E_F after the current drop. The ionic and electrical conductivity as well as the thickness of the film were identified as further key parameters for passivation. j_K reaches values bigger than zero only if the passive layer naturally dissolves and further oxidation of formed metal atoms can take place. According to Vetter j_K can be regarded as a measure for the passivation rate [15,16].

Passivation of zinc came into the focus of science only in the middle of the 20th century when the importance of zinc-based batteries became evident [1,17–19]. A comprehensive overview of corrosion and electrochemistry of zinc has been published by Zhang [20], but zinc passivation in alkaline media was just a short part of this work. Further general reviews of zinc passivation have been published by Liu et al. [21], by Armstrong and Bell [22] and by Smith [23]. However, in these contributions particular aspects of the topic such as the optical appearance of electrodes or specific investigation methods were considered. A more extensive summary of the acquired knowledge of the zinc passivation process as well as a summary of future research needs is the aim of the present review.

2. Chemical nature of the passive film on zinc in alkaline solutions

Huber [14] was the first who studied the passivation process of zinc electrodes in alkaline solutions. He considered that anodic passive films on zinc would have several properties advantageous to analytical work. Firstly, zinc forms ions of one single valence, secondly, the passive layers on zinc are clearly visible so that investigations with simple optical methods are possible. Furthermore, compounds of zinc often transform into a crystalline state, thus X-ray diffraction (XRD) measurements can be done to identify the anodic products.

Huber detected that a passive layer starts to cover parts of the electrode during the active dissolution of a zinc electrode in 1 N KOH solution. With increasing concentration of anodic products in the vicinity of the electrode, the passive layer transforms to a coherent film which prevents further zinc dissolution, the electrode becomes passive. XRD analyses showed that the passive layer mainly consisted of γ-zinc hydroxide with only a small fraction of zinc oxide [14,17]. At higher KOH concentrations zinc hydroxide could be no longer detected and the passive layer is only composed of zinc oxide. A good overview about properties and crystal structures of zinc oxides and hydroxides was published by Armstrong and Bell [22]. Some studies are devoted to the semiconductive n-type behavior of passive films on zinc [24–29].

The results of Huber were confirmed by further research groups [30–33] through application of optical and electron microscopy as well as electron diffraction. Nikitina [33] carried out an extensive study of passivated zinc electrodes by means of microscopy and X-ray diffraction. Both prismatic γ-zinc hydroxide and rhombic ε-zinc hydroxide as well as zinc oxide were identified, depending on KOH concentration and temperature. The changing nature of passive films at different KOH concentrations is most likely due to the presence of different zincate species at the corresponding pH values [27] (Fig. 2). At temperatures below 0 °C and lower alkali concentrations γ-zinc hydroxide was found to be the predominant species. At room temperature ε-zinc hydroxide usually forms on the electrode. However, Nikitina observed that prismatic zinc hydroxide did not lead to passivation of zinc. The electrode became passive at the start of transition of γ-zinc hydroxide to the rhombic modification due to its higher stability at increasing temperature and saturation. Nikitina concluded that ε-zinc hydroxide was in most instances responsible for the formation of passive films. Euler [34] proposed the formation of zinc peroxide and reported a positive iodide test for peroxide, although there is no X-ray evidence for the presence of zinc peroxide in the passive film [17]. On the other hand, peroxide formation on corroded metal surfaces has been described in the field of corrosion science at a very early stage [35,36].

One of the most noticeable characteristics of the passive layer on zinc is its variable coloring. Huber [14] investigated the physical appearance of passive films at different alkali concentrations (Table 1). He reported that the coloring of the film was more

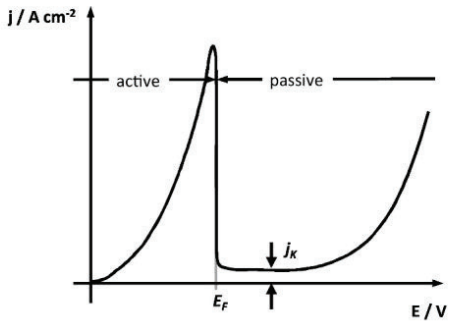

Fig. 1. Potential-current characteristics of a metal electrode with transition from active to passive state (after Vetter [15]).

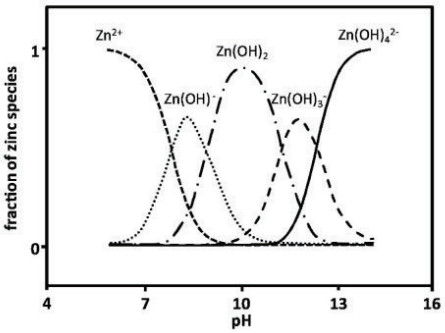

Fig. 2. Distribution of zinc species in alkaline solution as a function of pH at 25 °C (after Macdonald et al. [27]).

Table 1
Visible coloring of passive layers on zinc in unstirred alkaline solutions [14].

Electrolyte concentration	4 N	1 N	0.5 N
coloring		light beige	light grey violet
	light brown-yellow	violet-brown	brown violet
	light brown	violet-black	brown black

dependent on the flow conditions of the electrolyte and the electrode potential than on the composition of the electrolyte.

Hull et al. [37] observed the change of the passive layer during cycling anodic polarization in quiescent 5 N KOH solution and summarized their findings in Fig. 3. At the beginning of the measurement, the current density increases linearly with the potential and the electrode remains bright. When the current density reaches the maximum, a milky white film begins to form. During further polarization of the electrode, the surface under this film can be observed to darken until a region of intense current oscillation is reached. At this point, the film appears black; however, at more positive potentials the color rapidly lightens and a white and crystalline passive layer covers the electrode.

In addition, Huber [14] described the structure of the passive film. He observed zinc oxide on the electrode developing layers, which transformed to scales forming a porous covering. Huber determined optically a rather low value of 0.8% for the porosity of the covering.

Fry and Whitaker [38] also took a closer look at physical properties of the passive layer on zinc. They used microsections for measuring the thickness of the passive films and reported an average value of 4.0 μm. The density of the passive film, measured by weighting isolated film of known area, was in the range of 1.8–3.5 g/cm^2. The porosity was about 45% with pore sizes of about 500 Å, determined by direct transmission electron micrographs. The electrical resistance of black film calculated from anode potential and current was around 10 Ω cm, while the resistance of white film grew up to 1000 Ω cm. Several groups assumed the presence of finely divided metallic zinc in the passive layer which could lead to the black appearance of the electrode [10,33,38–41], but no conclusive evidence thereof has been provided. Powers and Breiter [40] confirmed results of Huber [14] and Hull [37] regarding appearance and growth of passive layer on zinc; however, they were the first who noticed the duplex nature of the film. Microscopic observation under quiescent conditions revealed a film formation similar to that reported by Hull, but in stirred electrolyte the milky coating near −1.27 V vs. Hg-HgO (Fig. 3) did not occur. Instead, a very different kind of film was observed which appeared much more compact than the first type. It ranged in color from light gray to black and seemed to form directly on the surface

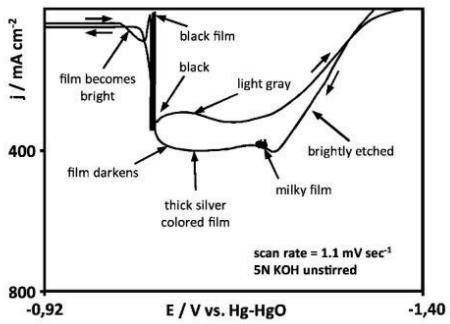

Fig. 3. Formation and change of the passive film on a zinc wire electrode during cyclic polarization in unstirred 5 N KOH solution recorded at a scan rate of 1.1 mV/s (after Hull et al. [37]).

of the electrode. According to this finding, the film that forms on a zinc electrode under quiescent conditions must be of a duplex character. A porous white film type 1 covers the dense film type 2. In the presence of convection, only type 2 film is observed to form.

Further working groups investigated the passivation of zinc in alkaline solutions by application of spectroscopic methods [5,23,42,43]. Hugot-Le Goff et al. [42] used an electrochemical cell with 2 mm electrode distance and 5 M KOH + 0.5 M ZnO electrolyte, which allowed in-situ measurements under a Raman microscope (argon laser, 514.5 nm, 200 mW). Afterwards polarization curves were measured and Raman spectra at relevant points of the polarization were recorded. Contrary to Huber [17], Hugot-Le Goff et al. could observe the formation of zinc hydroxide only in corrosion experiments with pure zinc in slightly alkaline electrolytes [44]. During anodic dissolution of zinc at higher pH values ZnO was found to be the main constituent of the passive film in the entire potential range. Nevertheless, these results confirmed the suggestion of Powers and Breiter [40] about the dual structure of the film. Near the dissolution peak of the polarization curve, passivation would be induced by precipitation of zinc oxide from a supersaturated zincate electrolyte. In the passive range film formation would occur due to the growth of a zinc oxide layer by a solid-state mechanism.

In a more recent publication of Mokaddem et al. [45] the authors described three different types of passive films which formed on the surface of zinc anodes in slightly alkaline electrolytes during chronoamperometric investigations. Type 1 film appeared due to the local saturation of electrolyte with zincate ions in the vicinity of the electrode. Passive film type 2 formed on the zinc surface underneath the film type 1, as it was described in previous work. However, Mokaddem et al. measured only a slightly inhibiting effect of passive type 1 and type 2 films on the dissolution of zinc anodes. The transition to the passive state finally occurred after the formation of the passive film type 3, although the amount of oxide necessary to passivate the surface was significantly less than formed during the type 1 and type 2 stages.

Cai et al. [5] investigated the passivation process of zinc using in-situ Raman spectroscopy (532 nm) on a commercial AA Zn-MnO_2 battery. They found out that the maximum usable capacity of the battery decreased with rising discharging current density. It was shown that this undesirable phenomenon was caused by the formation of a passive film on the zinc particles. In agreement with Hugot-Le Goff et al. [42] only ZnO and no $Zn(OH)_2$ was detected. In conclusion, the results of various working groups show that the passive film consists of zinc oxide. The black coloration of the passive film was attributed to an excess of zinc in zinc oxide.

3. Mechanism of anodic zinc reactions

3.1. Mechanism of active zinc dissolution

To understand the reason and the process of zinc passivation, it is necessary to consider the reaction mechanism of active zinc dissolution. Several groups studied the zinc dissolution kinetics in alkaline electrolytes by application of rotating-disc electrodes [46–49]. One of the most important works was published by Bockris et al. [49], who used a specially designed measuring cell which was

described in detail elsewhere [50]. Bockris determined Tafel parameters from his measurements and found Tafel slopes to be independent of the solution composition with anodic transfer coefficients of 1.3 ± 0.35. The anodic reaction order for zincates was determined to be 0.06 and the reaction order for hydroxide ions 2.59.

Based on the assumption that the simplest reaction mechanism must consist of at least four steps, the formation of the complex ion, with two steps including a charge transfer, a possible reaction path was suggested. The rate-determining step (rds) was identified from the Tafel parameters considering the theory of multistep electrode reactions [49].

$$Zn + OH^- \leftrightarrows ZnOH + e^- \quad (I)$$

$$ZnOH + OH^- \leftrightarrows Zn(OH)_2^- \quad (II)$$

$$Zn(OH)_2^- + OH^- \leftrightarrows Zn(OH)_3^- + e^- \text{ rds} \quad (III)$$

$$Zn(OH)_3^- + OH^- \leftrightarrows Zn(OH)_4^{2-} \quad (IV)$$

In contrast, Mokaddem et al. [45] published considerably lower values for the reaction order for hydroxide ions of 1.4–1.8 while in agreement with Bockris et al. the Tafel slope, which varied from 41 mV/decade at 0.1 M NaOH to 46 mV/decade at 1 M NaOH, was almost independent of the electrolyte composition. According to their experimental results and the observed formation of at least three types of passive films (cf. Chap. 2), this group proposed an alternative mechanism of active zinc dissolution, considering the formation of adsorbed zinc hydroxide intermediates:

$$Zn + OH^- \leftrightarrows ZnOH_{ads} + e^- \quad (V)$$

$$ZnOH_{ads} + OH^- \leftrightarrows Zn(OH)_{2(s)} + e^- \text{ rds} \quad (VI)$$

$$Zn(OH)_{2(s)} + OH^- \leftrightarrows Zn(OH)_3^- \quad (VII)$$

$$Zn(OH)_3^- + OH^- \leftrightarrows Zn(OH)_4^{2-} \quad (VIII)$$

Further mechanisms of active zinc dissolution, which however have not received considerable attention, were proposed in [51–55]. Cachet et al. [51,56] criticized the use of short-time measurements for studies of the zinc dissolution mechanism because they would not be sufficient to predict the steady-state behavior of zinc electrodes. Therefore, the authors described zinc dissolution in the following way:

$$Zn \leftrightarrows Zn^I + e^- \quad (IX)$$

$$Zn^I \leftrightarrows Zn(OH)_4^{2-} + e^- \quad (X)$$

Here, Zn^I stands for a monovalent zinc intermediate such as ZnOH or $Zn(OH)_2^-$. This mechanism permits the possibility of interfacial layer formation, which depends on electrode potential and electrolyte composition. The Tafel slopes measured by Cachet et al. [56] were with 10 mV/decade much lower than the values reported by Bockris et al. [49] and Mokaddem et al. [45].

3.2. Mechanism of passive film formation

The mechanism of zinc passivation is not fully understood, but three different theories of film formation on the zinc surface were postulated: the "dissolution-precipitation" model, the "adsorption" model and the "nucleation and growth" model [21,57–59]. Passivation processes according to "adsorption" or "nucleation and growth" models are often described as "solid-state" reactions. It has been intuitively assumed that the composition of the electrolyte in the vicinity of the anode is the factor determining the onset of film formation by one of the possible mechanisms [60].

3.2.1. The "dissolution-precipitation" model

In the "dissolution-precipitation" model [61–63] zincate ions build up in the in the vicinity of the electrode until their concentration reaches a critical value and zinc salt precipitates onto the electrode. The passivating film hampers the further zinc dissolution, resulting in the rapid rise in potential until oxygen evolution begins [60,63].

Armstrong [58] indicated that the nuclei of the precipitated material will always be three-dimensional so that the passivating film will not develop in monomolecular layers. Furthermore, the precipitate will form "near" the electrode surface and not directly on it. Dirkse [64] described the polymerization mechanism of zincate ions in the supersaturated region near the electrode. In solutions more concentrated than about 33 wt% KOH, there is insufficient water to completely hydrate the K^+ and OH^- ions. In these solutions zincate ions could release their water of hydration giving rise to polynuclear species of the type shown in Fig. 4, as the common zincate ion $Zn(OH)_4^{2-}$ is considered to have a tetrahedral configuration [22]. Addition of KF to KOH solutions leads to a faster passivation because KF removes water molecules by hydration and this loss of water lowers the mobility of OH^- ions [65,66].

As these polynuclear species form and grow they will eventually cause the formation of a precipitate on the electrode. In order to precipitate as ZnO, these species would first release OH^- ions and H_2O molecules. Thomas et al. [32] observed the formation

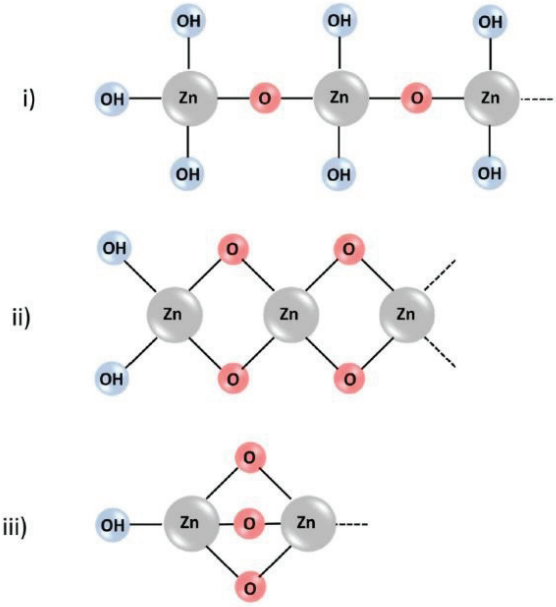

Fig. 4. Polymer zincate species (after Dirkse [64]).

of voids between the compact oxide layer and the electrode surface by cross-sectional electron microscopy of the passive layer, what finally confirms the assumptions of Armstrong and Dirkse [58,64].

Liu et al. [21,62] summarized in 1980 the scientific information about the dissolution-precipitation process of zinc passivation and proposed a three-step mechanism of the layer formation, which is schematically illustrated in Fig. 5. In the first step, the anodic dissolution of zinc proceeds for the time t_a producing zincate ions which accumulate near the electrode:

$$Zn + 4\ OH^- \leftrightarrows Zn(OH)_4^{2-} + 2\ e^- \quad (XI)$$

When the critical zincate concentration c_{crit} is reached, a passive layer begins to precipitate:

$$Zn + 4\ OH^- \leftrightarrows Zn(OH)_4^{2-} + 2\ e^- \quad (XII)$$

$$Zn(OH)_4^{2-} \leftrightarrows ZnO + 2\ OH^- + H_2O \quad (XIII)$$

Reaction (XII) was estimated to be first order with respect to the zincate ion concentration and to proceed much slower than reaction (XIII) [39].

The value of c_{crit} is estimated to be much higher than the solubility of ZnO in KOH solution [53,58,63,67]. However, the presence of zincate in the electrolyte shortens the passivation time, which will be discussed in Chap. 5.2. In contrast, a flow of electrolyte has a positive influence on the passivation time because of the removal of zincate ions from the electrode surface (Chap. 5.1).

As suggested by Armstrong [58] and Dirkse [64], the first passive layer does not cover the total surface of the electrode so that anodic dissolution continues through the porous film up to time t_b (Fig. 5). During the second step the diffusion of OH^- ions decreases up to a point at which no zincate ions can be formed and direct oxidation of the electrode starts.

$$Zn + 2\ OH^- \leftrightarrows ZnO + H_2O + 2\ e^- \quad (XIV)$$

If sufficient driving potential is available, the potential of the electrode rises to that required for the oxygen evolution:

$$4\ OH^- \leftrightarrows O_2 + 2\ H_2O + 4\ e^- \quad (XV)$$

The overall mechanism for the forward reaction can be represented as follows [57]:

$$\begin{array}{l} Zn(OH)_4^{2-} \longrightarrow Zn(OH)_2 \longrightarrow ZnO + H_2O \\ \quad\uparrow OH^- \\ Zn + OH^- \longrightarrow ZnOH^+ + 2\ e^- \\ \quad\downarrow \\ \quad ZnO + H^+ \end{array} \quad (XVI)$$

The dual structure of the passive film formed by precipitation on a zinc electrode was also reported by Szpak and Gabriel [61]. Depending on the conditions the coverings show a great variety of growth forms, investigated with a scanning electron microscope (SEM). Fig. 6 schematically illustrates the stages in the formation of the passive film. These observations confirm the previous findings of other working groups regarding the porous and polymeric structure of the first film. The SEM photographs of the passive layer show rolling or folding of the anodic film caused by internal stress developed in the course of film growth. The folding occurs when the oxide film reaches an estimated thickness of several hundred Å, opening an oxide free surface.

3.2.2. The "adsorption" model

In the "adsorption" model [37,40,53] passivation is assumed to occur when a certain anodic potential is exceeded. The film starts to form on the metal surface through the direct attack of the anion on the metal. The passivation proceeds on the basis of adsorbed intermediate $ZnOH_{ads}$ species (XVII). The anode transforms to the passive state when zinc ions can no longer diffuse through the oxide layer at a rate sufficient to support the required anodic current. The mechanism of "adsorption" theory can be described due to scheme (XVII) [57].

The formed film is non-uniform consisting of discrete nuclei which may be two-dimensional or three-dimensional in nature. After longer times these nuclei coalesce and form a continuous film, varying in thickness from one monolayer to thousands of monolayers. [58]

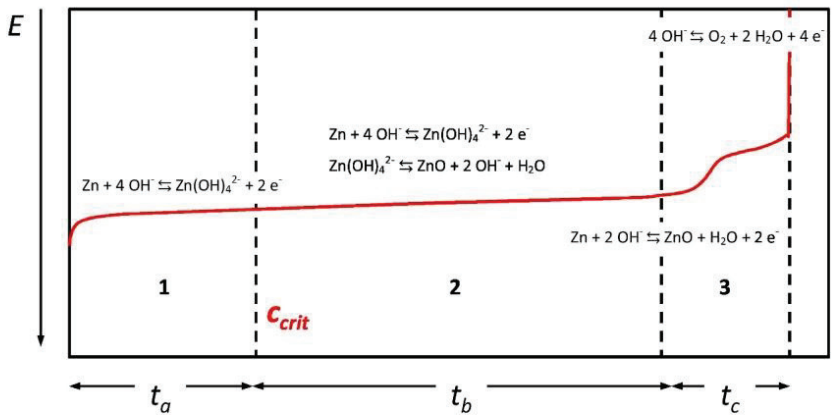

Fig. 5. Proposed scheme for the anodic passivation of zinc in alkaline solutions (after Liu et al. [62]).

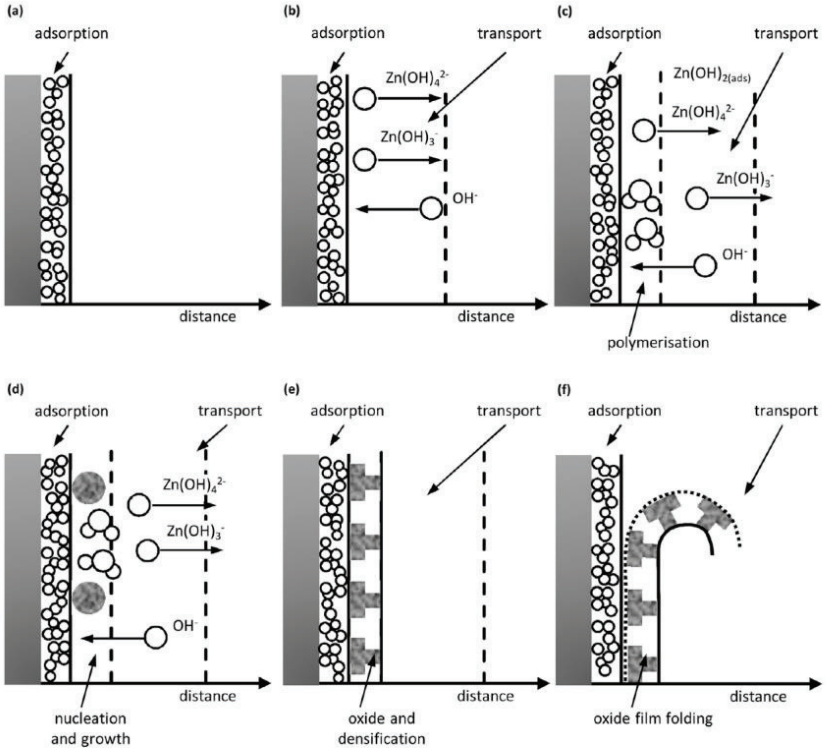

Fig. 6. Schematic representation of the development of anodic ZnO film: (a) quasi-equilibrium state; (b) development of transient region; (c) formation of polymerization region with trapping of monomers; (d) nucleation and growth region; (e) oxide densification; (f) oxide film folding (after Szpak and Gabriel [61]).

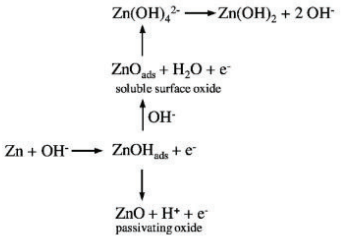

(XVII)

3.2.3. The "nucleation and growth" model

Like the "adsorption" model, the "nucleation and growth" model is based on the occurring passivation at a critical potential [68–71]. The passive film arises through formation of a monolayer resulting from the nucleation, growth and overlap of two-dimensional oxide clusters. The mechanism can be described with equation (XIV):

$$Zn + 2\ OH^- \leftrightarrows ZnO + H_2O + 2\,e^-$$

Kaesche [70] and Kabanov et al. [71–73] published that the electrode appears reversibly passive during anodic dissolution, even though the anodic quantity of charge equivalent to 1 mC/cm^2 would be sufficient to adsorb an approximately monomolecular oxide layer. This layer dissolves in alkali according to the adsorption model. With further passivation the thickness of the layer increases, following by growth of two-dimensional clusters which retard the dissolution of the metal.

When active metal dissolution occurs in parallel with the direct oxidation of zinc during the onset of passivation, the distinction is not easily made. Armstrong [58] as well as Baugh and Higginson [74] showed a measuring method for separate analysis of different passivation paths. For reversible metal dissolution the potential of the active-passive transition during ring-disc experiments would be expected to drift with the rotation speed for the dissolution-precipitation path, if the nuclei are formed at a sufficient distance from the electrode and can be swept away by the convective conditions at the disc. But there should not be any dependence of the active-passive transition on rotating speed during the direct oxidation of the electrode. This point will be more thoroughly discussed in Chap. 4.2.

4. Experimental investigations of zinc passivation

A number of working groups have studied the behavior of polycrystalline zinc electrodes in alkaline solutions with the aim to understand the passivation process and to determine the critical conditions at which the passivation occurs. Many groups [19,30,33,38,63,68,75–78] conducted galvanostatic studies of planar zinc electrodes. These studies give evidence of the relation between passivation time and current density, allow morphological observations of the passivation film and reveal information about the passivation mechanism. Another widely used method to investigate the dissolution process of zinc anodes are potentiostatic or potentiodynamic measurements [37,40,67], as it was already shown in Fig. 1. The resulting spontaneous decrease of the current density is understood as an indication of the critical potential of the electrode. Some groups used rotating disc

electrode (RDE) measurements [37,79,80] because of the advantage of precise setting of flow conditions or electrochemical impedance spectroscopy (EIS) [40,56,81] for investigations of kinetic properties of passivated electrodes. However, despite the high number of available measurement methods, investigations and results, there is little agreement among various descriptions of the zinc passivation process.

Sanghi and Wynne-Jones [82] concluded that the main influencing factors on the process of zinc passivation seem to be the anodic current density, the concentration and composition of electrolyte, the nature and purity of the anode as well as the duration of polarization. The investigations of zinc passivation are made difficult by two possible physical phenomena [82]:

a) Phase changes on the surface which may involve sudden changes in the internal potential drops between metal/oxide, oxide/solution and across the oxide layer.
b) Change in the mode of conduction from ionic to electronic (through interstitial ions, etc.), leading to a change in the nature of reaction on the electrode.

For that reason, Sanghi and Wynne-Jones stated that measurements based on constant current methods alone would not give the key information for understanding the passivation process.

4.1. Galvanostatic measurements

Landsberg [18] was one of the first who made extensive studies of the potential development of zinc electrodes in alkaline solutions during anodic dissolution with different current densities. He defined the passivation time as the duration of the measurement before the oxygen evolution occurred. Landsberg postulated the validity of the Sand Equation (1) [83] describing the relationship between current density and passivation time, referring to the work of Delahay et al. [84].

$$(i - i_c) = k \cdot t^{-1/2} \quad (1)$$

Here, i is the current density, t the passivation time, while i_c and k are model parameters. A more detailed description of the Sand equation will follow in Chap. 6.1.

Landsberg and Bartelt [19] observed that the passivation process was enhanced with decreasing alkali concentration during the anodic dissolution of zinc at a constant current density of 190 mA/cm^2. These authors identified three regimes which showed different relations between critical current density and passivation time (Fig. 7). The first two regimes are diffusion-controlled (Fig. 7a), so they can be mathematically described with the Sand equation (1). One can easily recognize in Fig. 7a that the transition from the first diffusion regime (lines) to the second one (dots) occurs at lower current densities for decreasing concentration of NaOH. In 0.5 N NaOH electrolyte the second diffusion-controlled area cannot be observed at all. For higher current densities a third regime with a linear relationship between current density and passivation time with i_1 and g as parameters (Fig. 7b) was observed [19]:

$$(i - i_1) = g \cdot t^{-1} \quad (2)$$

Considering the mechanisms of zinc passivation discussed in Chap. 3.2, the three dissolution regimes of Landsberg and Bartelt can be attributed to different processes of passive film formation. The diffusion-controlled regimes are an indication for the current density dependent rapid change of the effective degree of coverage of zinc. For the linear correlation regime it can be assumed that in this area the growth of the precipitate is the main process on the electrode. [19]

Despite the conclusions of Landsberg and Bartelt, many further research groups used equation (1) for describing their results obtained during galvanostatic dissolution of zinc even at very high current densities [53,76–78,85]. In some cases the measured passivation time was shorter than one second. In general, the passivation time has been understood as the duration of zinc dissolution until a rapid potential rise occurs, as it was shown in Fig. 5. Using the parameters i_c and k of equation (1) it is possible to develop correlations between the limiting current density and different influencing factors like KOH concentration and convection (Fig. 8). The results of Hampson and Tarbox (Fig. 8 a) reveal that the intersection with the abscissa, which has been defined as the limiting current density i_c, is close to zero, as it was also shown by Landsberg and Bartelt (Fig. 7). However, for non-horizontally positioned electrodes or for testing cells with natural or forced convection of the electrolyte, the values for i_c differ considerably from zero (Fig. 8 b) as shown by Brook and Hampson [85]. It was concluded from these results that passivation of zinc can be completely avoided by using flow cells.

As it will be discussed in Chap. 6a, the correlation $t^{-1/2}$ vs. i_c is based on the Sand equation, which is only valid for planar electrodes in quiescent solutions. It ceases to be valid once forced or natural convection starts. Consequently, the use of equation (1) for systems with vertical electrodes, like it was done by Brook and

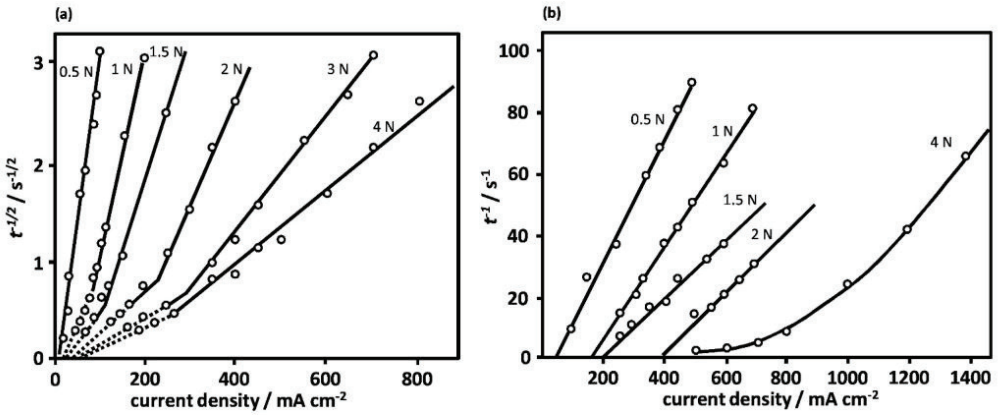

Fig. 7. Correlation between limiting current density and passivation time in NaOH solutions: (a) two diffusion-controlled regimes (lines and dots); (b) linear correlation regime (after Landsberg and Bartelt [19]).

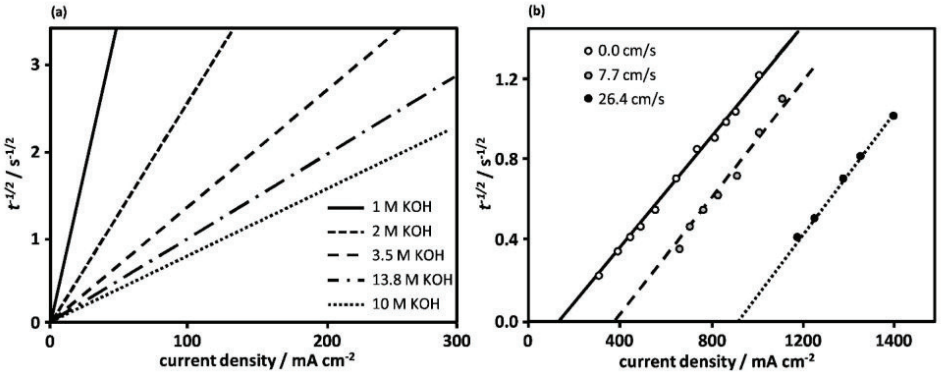

Fig. 8. Plots of (passivation time)$^{-1/2}$ vs. limiting current density for: (a) different KOH concentrations, horizontal zinc sheet electrode at 20 °C (after Hampson and Tarbox [75]); (b) for different electrolyte flow rates, 7 M KOH, 25 °C, cross-section of a zinc rod as anode, vertical position (after Brook and Hampson [85]).

Hampson [85], is not well founded. Nonetheless, the correlation $t^{-1/2}$ vs. i_c could be considered as an empirical relationship. It can be seen from Fig. 8b that the equation precisely describes the results of Brook and Hampson, which were achieved in a flow cell. However, these authors chose very high current densities during their experiments and drew conclusions about the limiting current density without measurements at lower currents. Fig. 9 shows that depending on the chosen relationship (1) or (2) between current density and passivation time the extrapolations of measured values of Brook and Hampson [85] at lower current densities exhibit two different trends. While the $t^{-1/2}$ vs. i_c line intersects the abscissa at a point different from zero so that this value can be interpreted as the maximum current density without passivation effects, the t^{-1} vs. i_c plot passes through the origin. That means according to the t^{-1} vs. i_0 correlation that even very small current densities would finally lead to passivation of the anode. Thus, additional measurements at lower current densities are required to confirm the determined value of the limiting current density i_c by Brook and Hampson.

Another critical point is that extremely high current densities of up to 1 A/cm^2 were applied, which are most likely higher than the maximum possible diffusion limiting current density of the system. Such high currents have no technical relevance and are not applicable in zinc based batteries. Furthermore several workers noted the lack of agreement between various investigations of galvanostatic zinc dissolution [30]. As an example, Fig. 10 clearly demonstrates drastic differences of passivation time results, although the working groups used similar electrode arrangements and conditions.

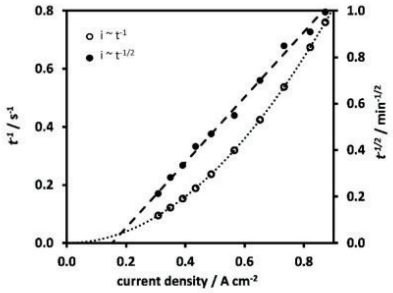

Fig. 9. Passivation time vs. current density plots of the results of Brook and Hampson [85] according to the Sand equation (1) and to the linear equation of Landsberg and Bartelt (2) [19], 7 M KOH, 25 °C, cross-section of a zinc rod as anode, vertical position and natural convection.

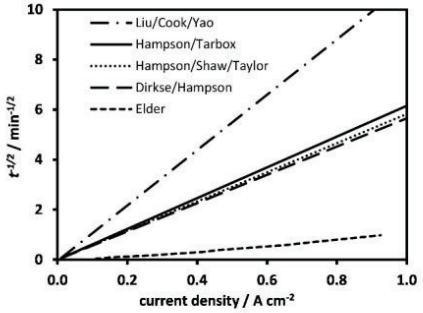

Fig. 10. Results of galvanostatic measurements of passivation time at various current densities from different workings groups, 6.5-7.25 M KOH without convection, 20-25 °C, horizontally orientated zinc sheet anodes [53,62,63,75,77].

4.2. Linear sweep voltammetry measurements

Several working groups [10,68,86–88] proposed linear sweep voltammetry (LSV) as a more valuable method for understanding the zinc dissolution process than galvanostatic investigations. During LSV a linearly increasing potential is applied and deductions about the passive layer formation can be made according to the resulting current response [37,40,59,68]. Fig. 11 shows a typical LSV current response curve with three peaks A, B and C, which arise at different overvoltages. Peaks A and B are overlapping and due to their high areas of considerable faradaic significance. It has to be noted that the scan rates influence the form of the peaks. At low scan rates peak A may become the minor peak, whereas with increasing scan rates peaks B and C weaken until peak C completely disappears.

Dirkse and Hampson [68] presume that every peak indicates a different process occurring at the electrode during anodic polarization. Overlap of peaks A and B means that both processes can proceed simultaneously. Furthermore, it was supposed that reactions occurring at the peak potentials are diffusion-controlled processes, since the peak current density is a linear function of the square root of the scan rate. The faradaic charge of peaks A and B corresponds to 10^3–10^{10} atomic layers which is too large for solid-state passivation reactions (Chap. 3.2). Several groups assumed the formation of $Zn(OH)_4^{2-}$ and $Zn(OH)_3^-$ to be responsible for the occurrence of peaks A and B [68,89]. Peak C, however, most likely indicates the direct formation of ZnO at the electrode surface. In

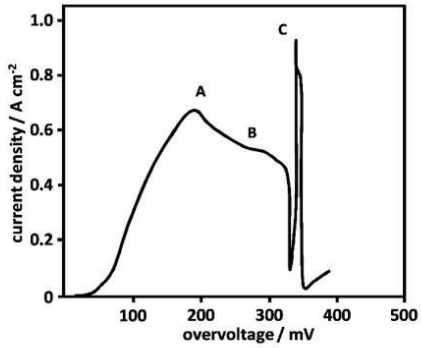

Fig. 11. LSV current response curve for horizontal zinc electrode, 10.2 M KOH, quiescent electrolyte, room temperature, scan rate 6.3 mV/s (after Dirkse and Hampson [68]).

general the onset of passivation is correlated with the sudden drop of current density to values of almost zero [68].

In addition to the scan rate, electrolyte composition, temperature as well as electrolyte convection also affect the shape of the LSV curves. Nevertheless, different working groups identified that the active dissolution of zinc always occurs up to an overpotential of ca. 0.16 V, while the passive region begins at an overpotential of ca. 0.30 V [37,45,59,68,90].

While in quiescent conditions reactions occurring at a zinc electrode are estimated to be diffusion-controlled, rotating disc electrode (RDE) measurements of Hull et al. showed that with increasing rotation speed diffusion control of the over-all reaction becomes increasingly less important due to the absence of linearity in the Levich plot [37,91]. These authors concluded that in case of high convection the passivation layer would form by adsorption of electrolyte anions rather than by precipitation processes. Further works of Cabot et al. [59] as well as Baugh and Baikie [80] or Barton and West [88] confirmed this conclusion.

Popova et al. [92,93] reported that during electrochemical dissolution of passivated electrodes in zincate saturated KOH solutions about 20% of the total electrical charge went into the thickening of the film. A more detailed quantitative assessment of the growth and breakdown of passive film under steady state-conditions based on LSV measurements was developed by Macdonald et al. [27,94,95], which will be discussed in Chap. 6.3.

Summarizing the results of LSV measurement it can be said that oxidation of zinc in quiescent electrolyte takes place via the dissolution-precipitation mechanism; however, exceeding of the critical potential initiates the solid-state reaction. Forced convection prevents the precipitation of a passive film while direct oxidation of zinc does not necessarily passivate the electrode. The rate of anodic oxidation of metal is limited by the rate of chemical dissolution of the film according to reaction (XIII) [92,95,96].

4.3. Electrochemical impedance measurements

One of the most important and informative investigations of zinc passivation has been made by Powers and Breiter [40]. Powers developed an electrochemical cell which allowed in-situ microscopic observation of zinc electrodes under polarization [97]. Two measurements of current density vs. electrode potential made on zinc specimens were combined with photomicrographs or with the determination of the ohmic and capacitive components of the electrode impedance (Fig. 12).

The characteristic shapes of parallel conductance $1/R_p$ and capacitance C_p, corrected by the electrolyte resistance R_{El}, as a function of the electrode potential can be correlated with the shape

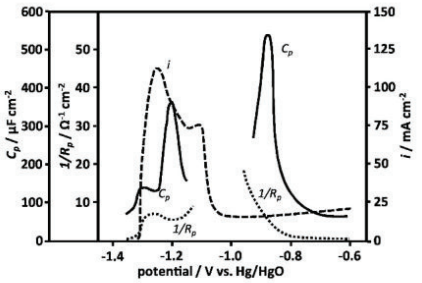

Fig. 12. Current density i, R_{El} corrected parallel conductance $1/R_p$ and capacitance C_p vs. potential for a cleaved zinc single crystal in quiescent 7 M KOH + 0.25 M ZnO electrolyte, horizontal position, scan rate 0.55 mV/s (after Powers and Breiter [40]).

of i vs. U plots. Both components of the impedance display a rapid change near the potential at which the current density undergoes an initial rise. The onset of passivation is correlated with an abrupt decrease of $1/R_p$ and a small increase of C_p. Powers and Breiter [40] pointed out that the measured values of the capacitance (up to several hundred $\mu F/cm^2$) were too high to represent the double layer. These values were rather attributed to a capacitance resulting from the presence of Zn_{ad}-OH^- species. Since two different capacitance maxima could be determined (Fig. 12), two different adsorption reactions were assumed to proceed in separated potential regions.

The results from electrochemical measurements confirm the optical investigations of Powers and Breiter [40] who postulated the formation of two different types of passive layer (cf. Chap. 2). Further working groups investigated the passivation of zinc by application of EIS [47,81,89,98–100]. Their results confirmed the findings of Powers and Breiter; however, the focus of these investigations was rather the determination of electrical properties of already passivated electrodes and not a closer examination of transition from active to passive states of zinc.

Very detailed EIS investigations of the zinc passivation process were made by Cachet et al. [100]. The rotating disc electrode made of zinc was galvanostatically polarized in 5 M KOH with 0.5 M ZnO at various speed rates until the electrode potential reached a constant value. EIS measurements were performed after reaching the steady-state in potentiostatic mode. The developed mathematical model based on EIS investigations, which enabled conclusions on the porous structure of the passive layer, the changes of kinetic properties of the electrode during dissolution, the diffusion of oxidation products and the concentration profiles of zinc species during electrode polarization will be discussed in more detail in Chap. 6.3. Based on simulation results Cachet et al. could prove their statement that active zinc dissolution would take place through a porous oxide-containing layer on the electrode. The determined diffusion coefficient of zincate ions at low electrode overpotential of 3 mV was with $1.5 \times 10^{-8}\,cm^2/s$ smaller than published values of previous groups and decreased to $0.6 \times 10^{-9}\,cm^2/s$ for a higher overpotential at the electrode of 15 mV. The electrode fraction covered by solid material θ and the resistivity ρ_m of the film increased from values of 0.3 and 600 Ω cm to 0.45 and $2 \times 10^5\,\Omega$ cm, respectively.

The work of Cachet et al. [56] is a direct contradiction to the proposed mechanisms of zinc passivation (Chap. 3.2). Due to low overpotentials at the electrode the solid-state reactions (cf. Chap. 3.2.2–3.2.3) could not take place. However, the group showed that an oxide-containing porous layer appeared on the electrode already during active dissolution of zinc. According to this finding, there is no need for reaching a critical zincate concentration (cf. Chap. 3.2.1) to initiate the zinc passivation process. Further

research effort is necessary to validate and extend the findings of Cachet et al.

4.4. Spectroscopic, optical and acoustic measurements

Several groups applied spectroscopic, optical and acoustic methods for in-situ investigations of zinc passivation and observations of the film growth. Nakata et al. [7] used operando X-ray fluorescence for monitoring of zincate ions distribution in the vicinity of the zinc anode during its anodic dissolution. Although in-depth studies have not been reported in this paper, the designed cell and the method could be applied to obtain new important knowledge about the passivation process.

Bhadra et al. [101] published a new electrochemical-acoustic method of anode characterization in zinc manganese dioxide AA alkaline batteries. The described method of electrochemical-acoustic time-of-flight analysis (EAToF) uses an ultrasonic transducer to generate an acoustic pulse which travels through the battery components. According to the specific chemistry and form factor of the cell, a unique waveform is received as output. In order to understand the EAToF measurements, correlation between acoustic results and SEM and energy-dispersive X-ray diffraction (EDXRD) have been considered. The authors were able to make first statements about the amount of ZnO within the cell and the morphology of the zinc anode. Further development of this method could provide an inexpensive and easily available technique for fast analyzing the state of health of zinc-based alkaline batteries.

Arise et al. [102] investigated horizontal upward-facing zinc anodes during electrochemical dissolution in 1.95 M KOH electrolyte at constant current density of 20 mA/cm^2. Morphological variations of the zinc surface were examined with the help of SEM after 0 s, 5 s, 100 s, 600 s, 3030 s and 15240 s of polarization. After 15240 seconds, the potential of the anode abruptly shifted toward positive values. According to SEM images, the zinc surface was completely covered with zinc oxide at this point. In order to prevent the electrode from passivation, the starting point of zinc oxide precipitation has therefore to be determined. Already after 5 seconds of dissolution, local aggregations of zinc oxide in polishing scratches on the zinc surface were observed on SEM images. During further oxidation of the zinc electrode these ZnO clusters continuously grew, filled the surface scratches of the electrode and finally formed a flocculent film. Once the anode surface was fully covered with this loose film, another type of precipitant grew on top of that film forming a crystallization network. At the end of the experiment, the SEM image of the electrode showed the appearance of a typical orthorhombic plate crystal layered structure of zinc oxide. Arise et al. determined the formation of the flocculent film on zinc after 600 seconds dissolution time at 20 mA/cm^2 as starting point of passivation. With the help of a two-dimensional mathematical model (Chap. 6.1) the authors estimated the critical concentration of zincate ions at the electrode surface to be 0.6–0.7 M. This concentration is nearly 5.5 times higher than the chemical and 1.3 times higher than the electrochemical solubility limit of zincates in 1.95 M KOH [103]. It is well known that a much higher concentration of zincate ions in KOH electrolyte can be achieved by an electrochemical dissolution of a zinc anode than by a chemical dissolution of ZnO [39,76].

Although the removal of zinc probes and their drying before the SEM investigations has certainly caused a transformation of the formed passive layer, Arise et al. [102] have chosen an interesting approach for zinc passivation studies and provided valuable results for determination of critical zincate concentration inducing the passive film formation.

Raman spectroscopy (Chap. 2) is able to deliver information about the structure and composition of passive films, but it was not able to show the starting point of passivation process.

An extensive study of the zinc dissolution process and the formation of oxidation products in alkaline electrolytes was made by Smith using ellipsometry [23], a surface-sensitive technique which can be coupled to electrochemical experiments to study surface reactions on metallic electrodes. In case of zinc passivation spectroscopic ellipsometry allows in-situ observations of rapidly growing anodic films and provides information about its physical properties. Smith investigated the influence of current density and of forced convection on the critical concentration of zincate ions leading to total passivation of the electrode. Fig. 13a shows the model of formation of several passivation layers on the electrode used to explain the results of ellipsometry measurements.

Although Smith [23] described the observation of the starting point of passive layer formation on zinc and determined the layer thickness, graphical visualization of his results shows essential discrepancies (Fig. 13b). Generally, it can be seen from Fig. 13b that higher flow rates lead to lower critical zincate concentration required for passivation, which is somewhat surprising. Furthermore, this trend is not apparent for every applied current density. Smith explained that lower convection would lead to very compact passive films, while at higher convection a more porous film would grow. A better mass-transport rate of zincate ions at higher

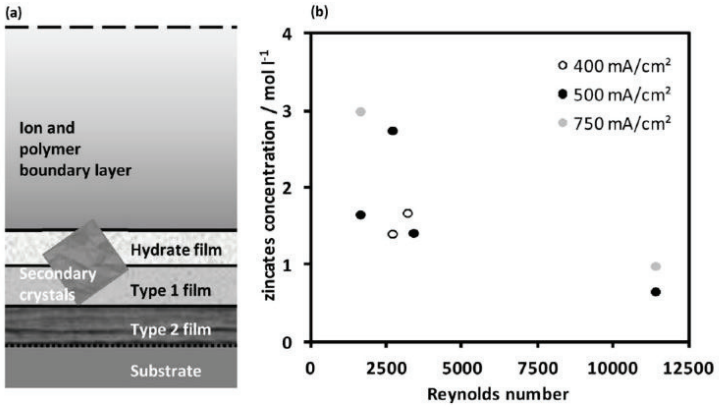

Fig. 13. (a) Optical model for interpretation of ellipsometric measurements of zinc passivation; (b) interfacial concentrations of zincate ions leading to passivation of the electrode in 6.01 M KOH, derived from ellipsometric measurements (after Smith [23]).

Reynolds numbers would reduce the concentration in the vicinity of the electrode surface. Consequently passive film formation would proceed at lower zincates concentration for higher electrolyte convection. In order to verify the conclusions of Smith it would be advisable to consider not only the zincate concentration as a cause for passivation, but also the overpotential of the electrode.

Further studies of passive film growth of zinc in alkaline electrolytes with the help of ellipsometry were published in [104–106]. However, the focus of these works was rather on physical properties of passive films and not on determination of the starting point of the passivation process. Influence of experimental parameters on zinc passivation process.

5. Influence of experimental parameters on zinc passivation

5.1. Influence of convection

Several groups investigated the variation of passivation time in dependence of the position of zinc anodes in the testing cell [21,76,85]. Vertical or downward facing positions of the specimen lead to a higher natural convection near the electrode surface than the upward position. Fig. 14 shows passivation times of upward and downward facing as well as vertical electrodes discharged at current densities ranging from 0.088 A/cm^2 to 0.629 A/cm^2. It is noticeable that for passivation times less than 25 s, all positions of the electrode show a similar correlation between passivation times and current densities. However, for passivation times longer than 25 s, the facing-downward and vertical positions enable a longer dissolution duration at a given current density. Since the density of KOH solution increases with increasing zincate concentration, natural convection can easily develop at the surface of the facing-downward and vertical electrodes. The facing-upward position of the electrode suppresses this natural convection and leads to a faster passivation.

The curves in Fig. 14 asymptotically approach different current densities. Eisenberg et al. [76] concluded that these current densities would be the critical values, which could be related to appropriate convection conditions without causing passivation.

Sanghi and Fleischmann [67] investigated the influence of forced convection on the passivation process of zinc during linear polarization measurements. As shown in Fig. 15, the current density increases with rising potential at the beginning of the experiment, but soon reaches a maximum value. This peak grows for higher concentrated alkaline solutions what means that the limiting current is caused by the insufficient rate of OH^- ions diffusion. Additional work has confirmed these results [88].

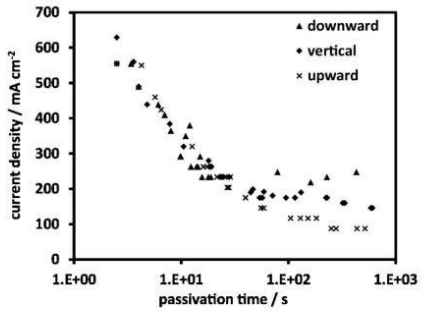

Fig. 14. Dependence of the passivation time on the electrode position in 6.924 M KOH electrolyte at room temperature (after Eisenberg et al. [76]).

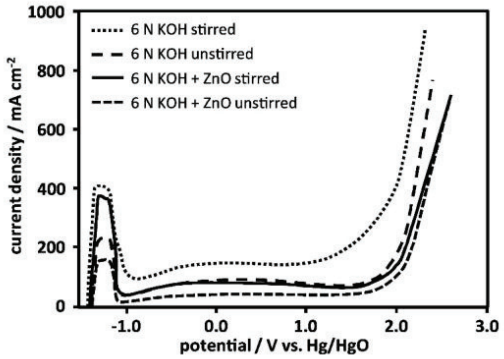

Fig. 15. Influence of forced convection on the passivation process of zinc in 6 N KOH electrolyte during linear polarization with a scan rate of 0.1 V/min (after Sanghi and Fleischmann [67]).

5.2. Influence of electrolyte composition

As already described in Chap. 3.2.1 passivation occurs at a critical concentration of zincate ions which is higher than the solubility of ZnO in KOH solution. The knowledge of the composition of electrolyte layers next to the electrode is therefore of decisive importance. Hampson and co-workers suggested in some of their publications that passivation proceeds when the concentration of zincates at the anode is equal to the hydroxyl concentration in the bulk [53,63,85]. In other publications these authors concluded that the critical value of zincates concentration is equal to half the concentration of hydroxyl ions [63,86]. However, the reason for the different values of critical zincates concentration was not discussed.

From investigations of Nikitina [33] it can be seen that there is an optimum for the concentration of KOH solution, at which the critical current density, which leads to passivation within 5 minutes, reaches a maximum. In Fig. 16a the results of Nikitina are superimposed with the values of specific conductivity of KOH for different concentrations at a temperature of 0 °C. It is noticeable that the conductivity of KOH has a direct influence on the critical current density and the 7 M KOH solution is obviously the ideal concentration for the zinc dissolution process. This conclusion is confirmed by the results of Dirkse [39] and Hampson et al. [30] who showed that the maximum limiting current in KOH solution occurred at a concentration of 20–30 wt% or 7 M. Dirkse considered that the reason for the decrease of the limiting current density at higher concentrations of alkali was the increase of viscosity which hampered the mobility of zincate ions. Zincate ions reduce the specific conductivity of KOH solutions and should have a negative influence on the passivation time of the anode. This relationship (Fig. 16b) has been proven by several groups [21,39]. The weakening of the influence of zincate ions on the limiting current density at less concentrated solutions can be explained by the poor solubility of ZnO. The amount of zinc in the electrolyte increases with rising pH value [39].

Landsberg and Bartelt [19] investigated the influence of salt additives in NaOH electrolytes on the duration of active zinc dissolution. In Fig. 17 the positive effect of NaCl in 0.5 N NaOH solution can be easily recognized. Similar results were achieved with Na_2SO_3 and Na_2SO_4 [19], $Na_2B_2O_7$ [27], $NaClO_2$ and NH_4Cl [80] or K_2SiO_3 [103,109]. The explanation of physical properties of salts in alkaline solutions during anodic dissolution of metallic electrodes was given by Vanyukova and Kabanov [110] and Macdonald et al. [95], who identified the adsorption of added anions at the zinc surface as the main cause for passivation suppression. Yang

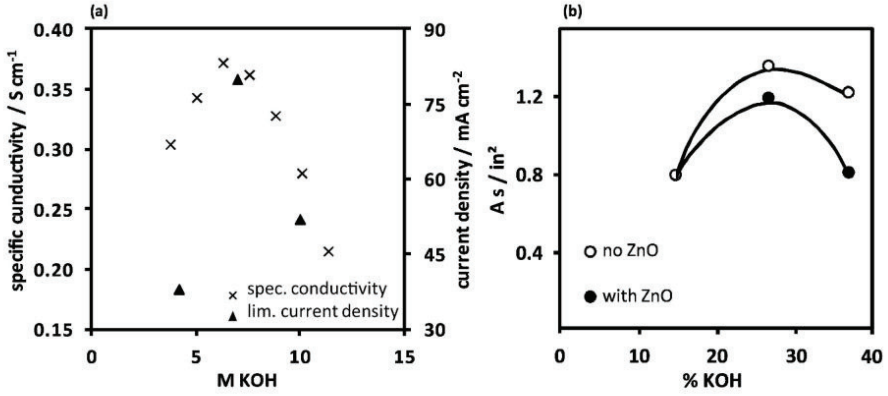

Fig. 16. Influence of KOH concentration on the limiting current density: (a) superimposition of specific conductivity of KOH and the limiting current density for different electrolyte concentrations at 0 °C (after Nikitina, Gilliam et al. and See et al. [33,107,108]); (b) dependence of the limiting current density on the concentration of pure and ZnO containing KOH electrolytes (after Dirkse [39]).

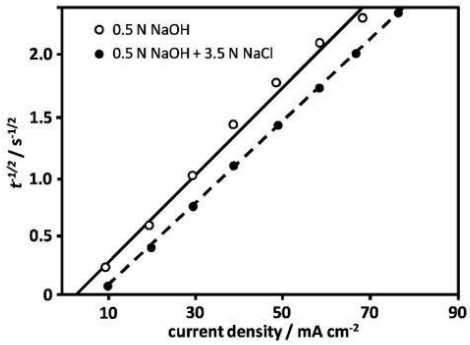

Fig. 17. Correlation between limiting current density and passivation time for zinc electrodes in 0.5 N NaOH solution with and without NaCl (after Landsberg and Bartelt [19]).

et al. [111] described the positive effect of dodecyl benzene sulfonate (SDBS) in alkaline electrolyte on the discharge capacity of zinc anodes. Due to addition of SDBS, the observed passive layer on zinc had a more porous structure, which allowed a better diffusion of formed zincates from the electrode surface. However, a total avoidance of zinc passivation with the help of electrolyte additives could not be demonstrated. A comprehensive overview of further passivation suppressing additives in alkaline electrolytes is given in [112].

As described earlier (Chap. 4.3), the current density increases during linear polarization experiments with rising potential up to a point at which the diffusion of OH^- ions becomes limiting and the rise of current density stops. Sanghi and Fleischmann [67] investigated the maximum value of the current density in dependence of the electrolyte composition. They assumed that ZnO would reduce the concentration of free OH^- ions in KOH solution so that the limiting current density would decrease. Due to the poor solubility of ZnO, zincate would show no effect in 0.01 N KOH solution and the largest difference in 6 N KOH electrolyte. Against the expectations, the greatest effect of ZnO could be observed in 0.1 N KOH. Sanghi and Fleischmann concluded that zincate ions did not exert only an influence on the available free OH^- ions but also on the occurring reactions. Some of these can be accelerated and others retarded by zincate ions under certain conditions.

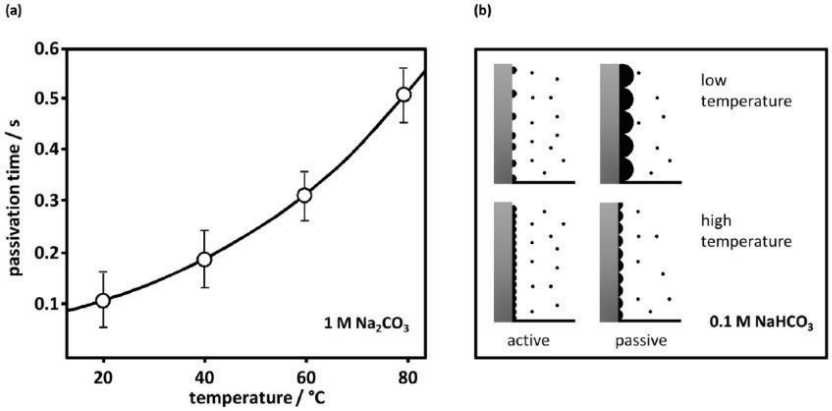

Fig. 18. (a) Influence of temperature on the passivation time τ_p at 10 mA/cm² in 1 M Na_2CO_3; (b) growth of passivating oxide, assuming a small number of oxide nuclei at low temperature and a high number at high temperature in 0.1 M $NaHCO_3$ (after Kaesche [70]).

5.3. Influence of temperature

Kaesche [70] observed the variation of passivation time of zinc electrodes (99.99% Zn) in different alkaline solutions. He pointed out that the influence of temperature on the behavior of the electrode in $NaHCO_3$ solution departed from the influence of temperature in a more alkaline solution of Na_2CO_3. While the passivation time increases with higher temperature in Na_2CO_3 solution as shown in Fig. 18a, zinc passivation shows the opposite behavior in $NaHCO_3$ solution. Kaesche observed that the zinc electrode in Na_2CO_3 becomes passivated in a very early stage of the dissolution process, so that the diffusion controlled supersaturation of the adherent layer of solution cannot be the reason for the potential drop. The transferred amount of charge approached only a value of 1 mC/cm^2 which is just sufficient to form a monomolecular layer of oxide.

In contrast to the observations in Na_2CO_3 solution, the passivation of zinc proceeds very slowly in $NaHCO_3$ solution. While during dissolution of zinc with 10 mA/cm^2 in Na_2CO_3 at 22 °C the potential drop took less than one second, the electrode could be discharged for 40 minutes in $NaHCO_3$ solution at the same current density. Kaesche postulated that the reason for the shortening of the passivation time in $NaHCO_3$ solution at higher temperature would be a marked decrease of the amount of oxide necessary for passivation. If the rate of growth of each oxide nucleus is approximately constant and the rate of nucleation increases with temperature, than the oxide layer at the moment of passivation will be the thinner, the higher the temperature is (Fig. 18 b). Kaesche stated finally that a similar behavior of zinc as in $NaHCO_3$ solution was also observed with 0.01 M NaOH.

According to the observations of Kaesche, the different behavior of zinc in 1 M Na_2CO_3 and 0.1 M $NaHCO_3$ solutions seems to be the result of disparate passivation mechanisms which proceed in alkaline solutions with various concentrations.

Nikitina [33] investigated the influence of temperature in highly concentrated KOH solutions on the critical current density at which the electrode passivates within 5 minutes (Fig. 19a). It is obvious that the critical current density rises with increasing temperature, as zinc oxide or hydroxide becomes more soluble in the electrolyte. Dirkse [39] and Hampson et al. [30] observed a similar relationship between temperature and the critical current density. Furthermore, the results of Nikitina show that for zinc probes with 1.5% mercury the critical current density reaches values comparable to anodes of pure zinc Fig. 19b.

5.4. Influence of interruptions

Dirkse [39] investigated the conductance of the electrolyte during anodic zinc dissolution and observed that the conductance decreased even when the current was interrupted (Fig. 20). It was concluded that a part of zinc oxide or zinc hydroxide, precipitated on the electrode surface, is slowly dissolved by the alkaline electrolyte. After an electrode had become passive, it would again become active if it remained in the electrolyte with no anodic current flowing. Several working groups confirmed this finding [18,30,60,74]. Hampson et al. [30], however, showed that the time for repassivation of a reactivated electrode was by far not as long as for a hitherto unpassivated anode. Landsberg and Bartelt [19] observed that short breaks with no current flowing during galvanostatic dissolution of zinc lead to a longer passivation time. The interruption of the measurement before the potential jump caused a nearly complete reactivation of the electrode, whereas zinc passivation after the occurrence of oxygen evolution was only partially reversible. Several working groups [18,37,81,95,104,105,113] noticed the possibility of cathodic dissolution of passive layers; however, Sanghi et al. [67,82] concluded from their observations that rather the hydrogen evolution would take place.

Investigations of the reversibility of zinc passivation showed contradictory results. It can be summarized, that, according to the dissolution-precipitation mechanism (Chap. 3.2.1) no reactivation of the electrode after a completed passivation process could be achieved. Short interruptions of the electrode dissolution lead to a temporary improvement of the electrode performance; however,

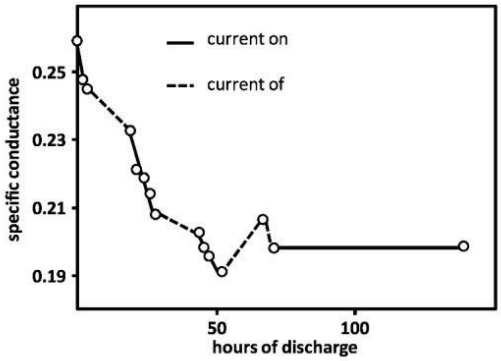

Fig. 20. Specific conductance of electrolyte during interrupted discharge (after Dirkse [39]).

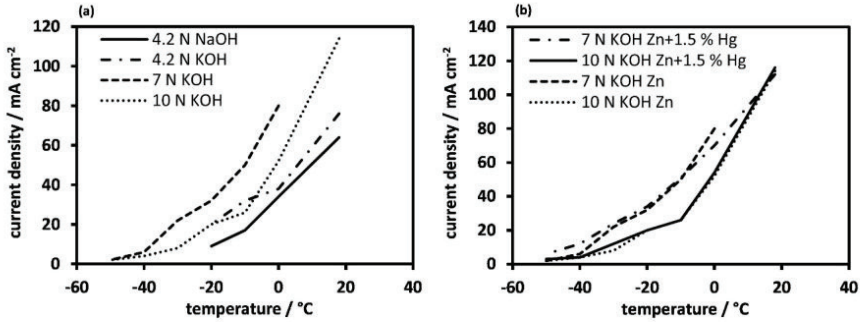

Fig. 19. (a) Influence of temperature on critical current density at which the anode is passivated in 5 minutes; (b) influence of Hg as an alloy component on zinc passivation (after Nikitina [33]).

full and prolonged reactivation could not be observed. On the other hand, during polarization experiments, which rather lead to thinner passive films according to solid-state reactions (Chap. 3.2), reversibility of zinc passivation could be noticed. Therefore, more extensive measurements have to be made to determine the influence of short interruptions at early stages of passivation during galvanostatic dissolution, as it was suggested by Landsberg and Bartelt [19], and to examine the influence of cathodic polarization of passivated electrodes. The dissolution of passive films on zinc could significantly prolong the passivation time or even prevent the electrode from passivation.

6. Modeling of zinc passivation

In the preceding chapters it has been shown that different theories for the formation of passive films on zinc surfaces have been developed. Consequently, no consistent theory as a basis for a mathematical model describing the passivation of zinc is available. However, the dissolution-precipitation mechanism is most commonly used as basis for mathematical modeling.

Physicochemical models can be divided by their dimensionality from 0-D up to 3-D (Fig. 21). 0-D models are without dimensionality, which means that only intensive values can be calculated. Passivation times would be such an intensive value which does not change with the size of the system. In models with higher dimensionality, geometrical properties of the electrode can be taken into account with increasing accuracy.

Over the years many models for zinc-air batteries have been developed. With gaining computational power these models became more complex and dealt with additional phenomena such as migration, structural changes of the electrode (Deiss et al. [114]) or with air composition and water level at anode and cathode to improve the operating strategies for zinc-air batteries (Schröder et al. [115]). However, only a few of these models take passivation effects into account, which are the main topic of this review. An overview about the different models for zinc passivation is listed in Table 2 sorted by the year of appearance.

6.1. Modeling of passivation times

Several authors used a simple mathematical approach which is based on a limiting surface concentration of zinc ions to calculate passivation times. It is assumed that precipitation and therefore the passivation of zinc oxide begins, if the surface concentration of zinc ions reaches its solubility maximum. The first equation of this kind was developed by Sand in 1901 [83]. He described the surface concentration during an unsteady-state diffusion process by a current density-time relation for systems without convective mass transport. It should be mentioned that Sand himself did not describe the passivation time of metals, but his approach was later used to describe the formation of oxides on the surface of metal electrodes and therefore could be used to predict passivation times. The equation was deduced from Fick's second law, where the analytical solution of Weber [129] was further developed to the one which is now known as the Sand equation. From the original Sand equation

$$c = c_0 - 2/\pi^{-\frac{1}{2}} zF(\pi/D)^{1/2} t^{1/2}, \tag{3}$$

and identifying the surface concentration c_0 as the critical precipitation concentration c_{crit}, one can obtain

$$i = \frac{1}{2}(c_{crit} - c)zF(\pi/D)^{\frac{1}{2}} t^{-1/2} = kt^{-1/2}. \tag{4}$$

Here, t is the time after which the electrode is completely covered and, therefore, is in the passive state, i the current, D the diffusion coefficient of the zincates, c the concentration in the bulk phase of the electrolyte, c_{crit} the critical concentration of zincate ions at which passivation occurs and z the number of electrons.

For further interpretation of the parameter k Liu et al. [62] considered the consumption of OH^- ions at the surface of the electrode. The supply by diffusion and migration is taken into account along with precipitation of ZnO. The thickness of the porous passive layer, which affects the supply of OH^- ions, is a function of time and current. By combining these assumptions with the Sand equation, a correlation for the k value was developed:

$$k = \left(\frac{\varepsilon^{(1+\tau)} D_b C_b}{\frac{\overline{V}_{ZnO} y}{(1-\varepsilon) n\boldsymbol{F}} \cdot \left(\frac{(4-2y)}{n\boldsymbol{F}} + \frac{t_0}{z\boldsymbol{F}} \right)} \right)^{\frac{1}{2}} \tag{5}$$

Here, ε is the porosity and τ the tortuosity of the porous ZnO layer, D_b the diffusion coefficient of OH^- ions, C_b the concentration of OH^- in the bulk, $\overline{V}_{ZnO}$ the partial molar volume, y the ratio of zinc precipitated as ZnO, t_0 the transference number, n the number of electrons involved in over-all electrode process and z the charge number of OH^- ions. It has to be noticed that n was used as fitting parameter and assumed values, which are not integers. Furthermore, the correlation (5) is only valid for current densities below 125 mA/cm^2. It was shown that values obtained from equation (6) and the Sand equation (1) are in the same order of magnitude. Liu et al. concluded that passivation is caused by a limited mass transport rate of OH^- ion across the porous ZnO layer.

Because of unavoidable additional mass transfer processes, e.g. natural convection within the cell, the current i was corrected by the limiting current density i_c, which is a measure for the non-diffusional mass transport and can be adjusted to the experiments [41]. Thus we obtain the Sand equation (1) in the already introduced form (Chap. 4.1):

$$(i - i_c) = kt^{-\frac{1}{2}}.$$

Although the Sand equation was developed for quiescent systems, Brook and Hampson [85] employed this relationship to interpret passivation times measured at different electrolyte flow rate. These authors found that k was not dependent on the flow velocity while i_c on the other hand was significantly influenced. They interpreted the term i_c in the Sand equation (1) for flowing systems by

$$i_c = 2FD(\Delta c)/d \tag{6}$$

where D is the diffusion coefficient, Δc the concentration gradient along the diffusion layer and d the thickness of the diffusion layer. Several other groups also showed that experimentally observed passivation times could be described by equation (1) [19,63,75,76] both for stirred and unstirred systems.

In summary, the Sand equation is an appropriate tool to describe passivation times with a simple mathematical approach. However, adjustment of parameters to specific experimental conditions is required. Further measurements of passivation times

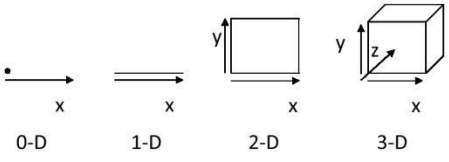

Fig. 21. Schematic visualization of model dimensionalities.

Table 2
Summary of mathematical passivation models ordered by their year of appearance.

Year	Authors	Mechanism of the passivation	Dim.	Important assumption	Calculated values or main outcome	Source
1900	Sand	–	0-D	Analytical solution of Fick's second law	Concentration of ions on metallic surfaces	[83]
1931	Müller et al.	Dissolution precipitation	0-D	Passivation as a time – current function	Potential and current at anodic peak	[13]
1961–1971	Eisenberg et al., Hampson et al., Bushrod et al.	Dissolution precipitation	0-D	Sand equation	Passivation times	[60,63,76]
1970	Brook and Hampson	Dissolution precipitation	0-D	Application of Sand equation to flowing electrolyte	Passivation times	[85]
1971	Dirkse et al.	Dissolution precipitation	0-D	Application of Sand equation to horizontal electrodes	Passivation times	[39]
1972	Farmer and Webb	Adsorption model	0-D	Sand equation not valid for forced convection	Passivation times at different electrolyte velocities and temperatures	[116]
1976	Despic et al.	Dissolution precipitation	0-D	*cece* mechanism	Dissolution mechanism of zinc with surface coverage	[117]
1979–2011	Macdonald et al.	Nucleation and growth	1-D	Bi-layer structure of the film	Growth and breakdown of passive films	[27,94–96,118]
1980	Sunu and Bennion	–	1-D	Porous electrode	Current distribution, potentials	[119]
1986	Cabot et al.	Dissolution precipitation	0-D	Ohmic controlled film growth	Potential and current at point of passivation	[120]
1981	Liu et al.	Dissolution precipitation	0-D	Different times for different passivation types	Passivation time, k value of Sand equation	[62]
1988–1991	Cachet et al.	Dissolution precipitation	2-D	Cylindrical pores	Dissolution of zinc trough a porous film	[51,56,100,121–123]
1990	Isaacson et al.	Dissolution precipitation	2-D	Porous electrode	Movement of active material from the center to the edge of the electrode	[124]
1992	Mao et al.	Dissolution precipitation	1-D	Porous electrode	Precipitation of potassium zincate	[125]
1986	Cabot et al.	Dissolution precipitation	0-D	Constant film thickness	Potential and current at point of passivation	[59]
2010–2013	Arise et *al.*	Dissolution precipitation	2-D	Single pore model	Passivation time, concentration profiles	[102,126]
2013	Song et al.	Dissolution precipitation	1-D	Porous electrode	Precipitation of zinc oxide	[127]
2014	Bosco et *al.*	Dissolution precipitation	1-D	Application of equilibrium constants for the species concentrations	Passivation time, concentration profiles	[128]

especially at low current densities are necessary to develop a physically founded interpretation of parameters.

As an alternative to the Sand equation, Farmer and Webb [116] developed a 0-D model for calculation of passivation times at high current densities (from 1.6 kA/m^2 up to 3.2 kA/m^2) in flowing electrolyte. The basis of this model is the formation of a passive layer initiated by a critical concentration of zinc ions at the electrode surface comparable to previous research. Additionally it was assumed that a laminar diffusion layer of thickness δ will form above the porous oxide layer. According to these authors, the following non-electrochemical reaction leads to passivation:

$$Zn + H_2O \rightarrow ZnO + H_2 \quad \text{(XVIII)}$$

However, this reaction is not in accordance with the different proposed passivation mechanisms described in Chap. 3.2. Diffusive mass transport occurs both through the laminar electrolyte film

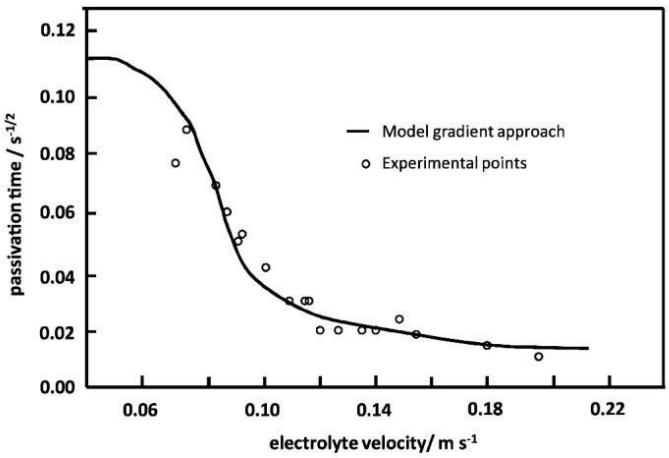

Fig. 22. Passivation times at different electrolyte velocities for 2.1 kA/m^2, calculated from [116] with the equations (7) and (8), parameters: $U_0 = 0.069\ m\ s^{-1}$, $\tau_0 = 102$ s, $a = 0.0193$, $D_2/D = 10$.

and the porous zinc oxide layer. With the following two equations

$$t_p = \frac{U_0}{U}\cdot\theta\cdot\tau_0, \tag{7}$$

and

$$a\left(\frac{D_2}{D}\right)^{\frac{1}{2}}\theta^{1/2} + \rho(\theta) = \sqrt{\frac{U}{U_0}}, \tag{8}$$

it is possible to calculate the passivation time t_p as a function of electrolyte velocity U. τ_0 is a time constant, adjusted to the experiments, D and D_2 are the diffusion coefficients of the zinc ions in the porous layer and the electrolyte, respectively, θ is the dimensionless time, $\rho(\theta)$ the normalized oxide/electrolyte interface concentration, a the 'oxide' growth constant and U_0 a reference velocity. It was furthermore shown that the passivation time at low flow velocities reaches a minimum value of

$$t_{min} = \frac{\pi}{4}\tau_0, \tag{9}$$

while at high flow velocities a maximum of

$$t_{max} = \frac{D}{D_2\cdot a}\tau_0 \tag{10}$$

is finally reached. Comparison between experiments and model for a current density of 2.1 kA/m^2 depicted in Fig. 22 reveals that the agreement is quite well, except for very low electrolyte velocities for which no experiments were conducted.

Two other more recent approaches for modeling of passivation times and zincate concentration profiles in alkaline zinc based systems were developed by Arise et al. [102,126] and Bosco et al. [128]. Arise et al. numerically calculated the zincate and hydroxide ions concentration profiles for a Zn-NiOOH battery cell. During the discharge of the cell hydroxide ions are consumed on the zinc electrode surface and formed on the cathode. According to the mass conservation and electroneutrality equation, the authors derived an expression for the governing electrolyte-phase equation for three different compartments: the zinc anode, the separator and the cathode. With the help of their model Arise et al. were able to calculate the anodic and cathodic current density distribution along the electrode surface [126], as well as the transient anode overpotential profiles and the concentration distribution of zincate and hydroxide ions. The group used experimental results from galvanostatic and SEM measurements discussed in Chap. 4.4 in order to validate the numerical model.

Bosco et al. [128] developed a dynamic one-dimensional model, which provides a new theoretical methodology for describing the time-dependent changes in the solution composition leading to passivity or pitting. Assuming that chemical reactions take place on much faster time scale than the diffusion of species, the species concentrations could be expressed with the equilibrium constants. Furthermore, the concentrations of the involved species were expressed by the corresponding atom concentrations of Zn, H and O and the resulting equation system was solved analytically considering three possible cases

i) diffusion and reaction in the semi-infinite medium
ii) diffusion and reaction in a finite diffusion layer as the rotating disc electrode
iii) diffusion and reaction in a thin electrolyte layer on the corroding metal

for free corrosion conditions and impressed current experiments. As results the space-time dependence of the various species concentrations and typical spatial concentration profiles were obtained. The advantage of the model of Bosco et al. [128] is its general applicability. The influence of further effects such as convection or migration on the concentration distribution can be easily complemented. The model can be adapted to different experimental conditions such as current density, pH value or use of additives in the electrolyte. However, no experiments have been performed yet to verify the model.

6.2. Modeling of electrochemical properties of the passive layer

The so far discussed models do not take into account the potential as a possible reason for passivation. This was shown by linear sweep voltammetry measurements, [37,40,59,68], which have been discussed in Chap. 4.2. Müller [13] published first equations to describe the passivation as a time-current function for metals in acidic solutions. In his numerous studies [130] he observed the nature of passivation layers, which build the basis for the models explained in this chapter. Müller's theory of current transient is based on two types of layer growth. Across the electrode surface a layer of constant thickness with low conductivity is assumed to form until only small pores in the layer remain. Subsequently, the layer thickness increases, while the pore diameter remains constant. The electrical resistance of the layer remains relatively small until a coverage of about 99% is reached. At this value the resistance increases abruptly and becomes rate controlling for the current flow [131]. Müller's works were first applied by Calandra et al.[131] and later used by Cabot et al. to describe the passivation of zinc in hydroxide solution in potentiostatic [59] and potentiodynamic [120] models. These authors extended the equations given by Müller for their used quiescent system.

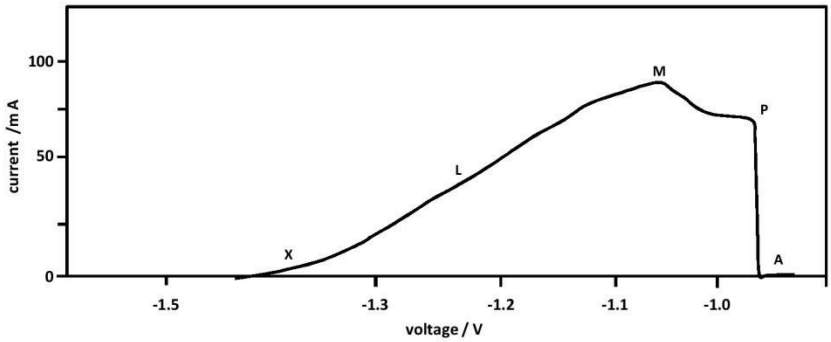

Fig. 23. Cyclic polarization curve of zinc in quiescent 4 M KOH solution at 5 mV s^{-1} (after Cabot et al. [120]).

The potentiodynamic model by Cabot et al. was introduced as "ohmic controlled film growth model". Fig. 23 taken from [59,120] shows the anodic polarization curve of zinc for a scan rate of 5 mV/s. After a linear increase of the current with rising potential (L) a region of pseudo passivity starts, where the current varies nonlinearly with the potential (M–P). Above this region one can see a drastic decrease of the current, reaching a region where the current is nearly independent of the potential. According to Cabot et al. the anodic peak (P) appears because of a lack of OH^- ions at the electrode surface, where passivation occurs below this potential. The application of Müller's model by Cabot et al. shows that precipitation of the passive layer might already appear in the linear I-E region (L), observed before the anodic peak.

Based on the works by Müller, Cabot et al. introduced equations to describe current I and potential E at the peak (M) and in the passive region (P) [120]:

$$I_{M/P} = \left(\frac{n \cdot F \cdot \rho \cdot k}{M}\right)^{1/2} \cdot S_0 (1 - \theta_{M/P}) \vartheta^{1/2} + I_{\vartheta=0}, \quad (11)$$

$$E_{M/P} = \left(\frac{n \cdot F \cdot \rho \cdot k}{M}\right)^{1/2} \cdot ((\delta/\kappa) + R_0 S_0 (1 - \theta_{M/P})) \vartheta^{1/2} + E_{t=0} \quad (12)$$

Here M is the weight of the film obtained with a charge of nF, ρ and δ are the density and the thickness of the passive film, κ the conductivity of the solution, S_0 the total area of the electrode, R_0 the resistance of the solution external to the film, $\theta_{M/P}$ the degree of coverage at the anodic peak and v the scan rate. Fig. 24 shows a good agreement between theory and experiments for different concentrations of potassium hydroxide.

Based on these models, the process of passivation can be described by the potential at the electrode where the insoluble film is built by a dissolution-precipitation mechanism [131]. In order to describe the observed current-time characteristics at a fixed potential, an additional potentiostatic model for the passivation was introduced by Cabot et al. [59], which is also based on earlier work of Müller [13]. In Fig. 25 a schematic of the experimental current-time curves for the passivation process is shown. One can observe an initial decrease of the current (a) with a following

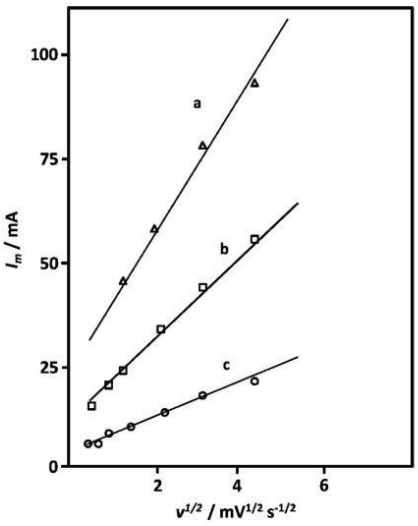

Fig. 24. Plots of limiting current I_m vs.(scan rate v)$^{1/2}$ according to Cabot et al. [120] with the adjusted equations of Müller. (a) 3.0 M KOH; (b) 2.0 M KOH; (c) 1.0 M KOH.

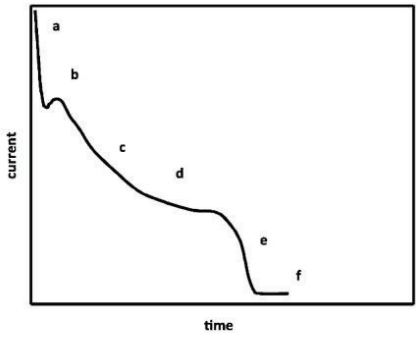

Fig. 25. Schematic of the experimental current vs. time curves (after Cabot et al. [59]).

maximum (b), a decay (c) followed by a current plateau (d) and a further decay with an inflexion point (f).

The model describing the final passivation stage in the region d-e-f in Fig. 25 considers that

i) the new phase grows via randomly distributed nuclei,
ii) the film, formed by dissolution-precipitation, has a constant thickness during the process,
iii) the dissolution and conductivity of the film are negligible and, therefore, the current passes only through non-covered areas,
iv) the non-covered areas continuously decrease in size to become small pores.

The correlation between current I and time t can then be described by [59]:

$$(t - \tau) = (A/I_i)[(-1/(1 - (I/I_i))) + \ln((I_i/I) - 1)]. \quad (13)$$

Here I_i is the initial current, A is a measure for the slope of the current decay and τ is the time at which the current plateau occurs. The results are compatible with the assumption of a porous film which blocks the diffusion process and consequently lower the performance of the electrode. However, for low KOH concentration (<0.5 M) the passive film was shown to grow as a monolayer (2-D growth). With rising KOH concentration the film tends to become thicker, which implies a transition to a 3-D growth mechanism resulting in a porous layer.

The so far discussed models deal with the passivation of planar zinc electrodes. The performance of porous electrodes (which are widely used in zinc batteries) under passive conditions are discussed in the following.

Isaacson et al. [124] developed a 2-D model of a porous zinc/zinc-oxide electrode in a secondary battery system with a NiOOH electrode as the counter electrode. The authors assumed that no convection would take place, thus only diffusion and migration were taken into consideration. Mass balances for the OH^- and $K_2(OH)_4^{2-}$ species were solved. It was assumed that the kinetics of the reaction can be expressed by a Butler-Volmer equation. Ohm's law with an integrated concentration gradient for each species was used to describe the conductivity of the electrolyte. A constant porosity of the zinc/zinc-oxide electrode during charge and discharge was considered. The precipitation process was described by an equilibrium reaction of zinc oxide and zinc hydroxide given in the chemical equation (XIII)

$$Zn(OH)_4^{2-} \leftrightarrows ZnO + 2\ OH^- + H_2O,$$

which is first order with respect to the OH^- ions concentration for precipitation and second order for dissolution. The critical concentration for the precipitation of zinc oxide was supposed to

be about 300% of the equilibrium concentration of $Zn(OH)_4^{2-}$ [132]. The total reaction rate r is expressed as the sum of the chemical and electrochemical reactions [124]

$$r = \frac{s}{nF}\nabla i_s + sk_p(c_3 - {c_2}^2/K_{eq}) \quad (14)$$

where s is the stoichiometric coefficient, i_s the current density in the electrolyte phase, c_3 the concentration of $Zn(OH)_4^{2-}$ and c_2 the concentration of OH^- ions. The equilibrium for zinc hydroxide and zinc oxide was given by

$$K_{eq} = \frac{k_p}{k_d} \quad (15)$$

with the reaction rate constants for the precipitation (k_p) and the dissolution (k_d) processes.

The model calculates electrode potentials, current densities, electrolyte concentrations and Zn and ZnO distributions after cycling of the cell. Movement of active and passive material during cycling was argued to occur because of asymmetries in the potential field caused by differences in the electrode geometry and concentration gradients, which also interfere with the reaction kinetics. This 2-D model shows the influence of active and passive material throughout the performance of the cell. The authors mention a sensitivity of Zn and ZnO redistribution to the exchange current density and the precipitation-dissolution rate.

Sunu and Bennion [119] developed a 1-D model for a primary zinc-air battery with a porous zinc electrode for which they predicted the current distribution, potentials in the solution, concentrations for hydroxide and zincate ions as well as porosity and volume fractions of zinc and zinc oxide as a function of time and position perpendicular to the surface of the electrode. One of the main features of the model is the calculation of capacity losses through pore plugging by precipitated ions and hydroxide ion depletion. To estimate the kinetic parameters, the mechanism by Bockris et al. [49] was considered. Mao and White [125] extended the model by Sunu and Bennion by a separator and the precipitation of ZnO and $K_2Zn(OH)_4$. The model is used to analyse and to maximise the performance of a primary zinc-air battery. The air electrode is considered to be a flat electrode with a high specific reaction area, due to its very low thickness in comparison with the zinc electrode. Caused by the extending volume of the precipitated solid potassium zincate, the mass transfer as well as the conductivity were limited through blocking the pores of the active material. The experimental results could be well described with the model.

Song et al. [127] developed a model, also based on the equations by Sunu and Bennion, for current densities in the range of 10–50 mA/cm^2. The upper current density limit was chosen in order to avoid a type 2 passivation film (Chap. 2), which was assumed to form only at higher current densities. Instead, a passive layer of type 1 occurring through the dissolution-precipitation mechanism was considered (Chap. 3.2.1). The film prevents the ions from diffusing to the surface, which leads to a potential drop. The modeling results demonstrate that the limitation of the mass transfer process by precipitation of zinc oxide has a significant impact on the electrode performance.

6.3. Kinetics and mechanisms of zinc passivation

Correct mechanistic interpretation of experimentally obtained parameters such as Tafel slopes and reaction orders requires the knowledge of the type of reaction mechanism involved. In the case of divalent zinc ions, several possible reaction paths are conceivable, which were already briefly discussed in Chap. 3.2 of this review. The present chapter is intended to provide a closer look at the mechanism of the passivation reaction and the active dissolution of zinc on passivated electrodes.

Despic et al. [117] investigated the kinetics and reaction mechanisms of active zinc dissolution that can lead to the full surface coverage. They suggested a reaction mechanism based on Bockris et al. [49] consisting of four steps. After each chemical reaction step (c) an electron-transfer step (e) follows resulting in a *cece*-type mechanism. Tafel plots obtained via galvanostatic anodic dissolution of zinc indicated that there is a limiting current density, which is not diffusion controlled. Based on the assumed reaction type, it was hypothesized that the limiting current density is due to the attaining of a full surface coverage by Zn^+. Therefore, the anodic current density should be proportional to the rate constant of the chemical reaction k and the surface coverage θ.

$$i = 2Fk\theta. \quad (16)$$

The model includes that the surface coverage Θ_{rev} at the reversible potential E_{rev}, which can be calculated with the Nernst equation, is low and the electrochemical step is fast compared to the chemical step. Then, the current can be calculated with the overpotential $\eta = E - E_{rev}$ by

$$i = 2Fk\Theta_{rev}\frac{\exp[a]}{\Theta_{rev}\exp[a] + \exp[a] + p} \quad (17)$$

with

$$a = \frac{(1-\beta)F}{RT}\eta, \quad (18)$$

where k is the chemical reaction rate constant, Θ_{rev} the reversible surface coverage, β the symmetry factor and p the ratio of chemical and electrochemical rate constants at the reversible potential.

Despic et al. discussed three characteristic regions for Eq. (17):

i) At low overpotential, where Θ_{rev} is low and the electrochemical step is fast, equation (17) becomes

$$i = 2Fk\Theta_{rev}exp\frac{F}{RT}\eta \quad (19)$$

with a Tafel slope of RT/F.

ii) At intermediate overpotentials, equation (17) becomes

$$i = \frac{2Fk\Theta_{rev}}{p}exp\frac{(1-\beta)F}{RT}\eta, \quad (20)$$

with a Tafel slope of $2RT/F$.

iii) At high overpotentials, Θ_{rev} becomes dominant and Eq. (17) can be simplified to

$$i = 2Fk = i_L \quad (21)$$

with i_L being the non-diffusion controlled limiting current.

The authors adjusted model parameters to experimental data and could prove the accuracy of the given equation. Therefore, the reaction mechanism of the *cece*-type originally proposed by Bockris et al., where the first reaction step is the rate-determining step, seems to be valid for zinc dissolution in highly concentrated potassium hydroxide.

Macdonald et al. introduced the so-called point defect 1-D model (PDM) for the growth and breakdown of passive films on metallic surfaces [95,96]. This model is based on the movement of point defects in an electrostatic field and enables the interpretation of growth behavior of a passive film on a metal surface and its possible local dissolution.

The PDM that describes the growth and breakdown of the passive film under steady-state conditions is based on following assumptions [96,133]:

i)

At a more positive external potential than the Flade potential (Fig. 1) a continuous passive film of oxide composition forms at the electrode surface.

ii) The passive film contains a high concentration of point defects.

iii) The passive film is an incipient semiconductor. Consequently, the electric field strength is a function of the chemical and electrochemical characteristics of the layer and is independent of its thickness.

iv) Electrons (e') and electron holes in the film matrix are in their equilibrium states and electrochemical reactions involving electrons are rate controlled at either the metal/film (m/f) or the film/solution (f/s) interfaces.

v) The rate-controlling step for process involving metal vacancies ($V_M^{x'}$) and oxide vacancies ($V_{\ddot{O}}$) is the transport of vacancies across the film. Therefore metal and oxide vacancies are in their equilibrium states at the m/f and f/s interfaces.

According to Macdonald et al. [96], the following reactions occur at the metal/film interface

$$m \leftrightarrows M_M + \chi/2\ V_O + \chi e' \quad \text{(XIX)}$$

$$m + V_M^{x'} \leftrightarrows M_M + \chi e' \quad \text{(XX)}$$

while two other reaction take place at the film/solution interface

$$V_{\ddot{O}} + H_2O \leftrightarrows 2H^+_{(aq)} + O_O \quad \text{(XXI)}$$

$$m \leftrightarrows V_M^{x'} + M^+_{(aq)}. \quad \text{(XXII)}$$

Here m represents the metal atom in the metal, M_M the metal cation in the film and O_O the oxygen ion in the anion site. Oxide ions vacancies are produced at the m/f interface but are consumed at the f/s interface. Therefore, oxide ions vacancies diffuse from the m/f to the f/s interface, resulting in oxide growth. The diffusion of $V_M^{x'}$ in the opposite direction results only in metal dissolution and not in the growth of passive film type 1 (Chap. 2). Macdonald et al. [96] indicated that this conclusion is opposed to assumptions of accepted theories that the diffusion of cation is responsible for the film growth. Consequently, the problem of calculating film growth kinetics can be solved by calculating the $V_{\ddot{O}}$ diffusional rate:

$$\frac{dL}{dt} = \frac{\Omega}{N_V} J_{V_{\ddot{O}}} \quad (22)$$

where dL/dt is the film growth rate, Ω the molar volume per cation, J_{V_O} the flux of oxide vacancies per unit area per unit time and N_v Avogadro's number. In order to solve this equation, values of the potential dependence of the potential drop $\varphi_{f/s}$ at the film/solution interface α, the pH dependence of $\varphi_{f/s}$ β, an intrinsic constant $\varphi_{f/s}^{o}$ and the field strength ε are required. Macdonald et al. determined numerical values of these parameters using experimental data of passive film formation on iron of previous work [96]. With the point defect model Macdonald et al. could show that α was independent of pH and anion identity in solution, whereas β was a strong function of the identity of anionic species. The potential drop at the film/solution interface was shown to be independent of the film thickness.

Similar to film formation, the diffusion of cation vacancies was shown to be responsible for the local breakdown of the passive film [95]. The cation vacancies move to the metal/film interface and tend to submerge into the bulk of the metal. However, when the cation diffusion rate is higher than the rate of $V_M^{x'}$ submergence into the bulk, cation vacancies start piling up and lead to appearance of voids at the metal/film interface. When the void grows to a certain critical size, the passive film suffers a local

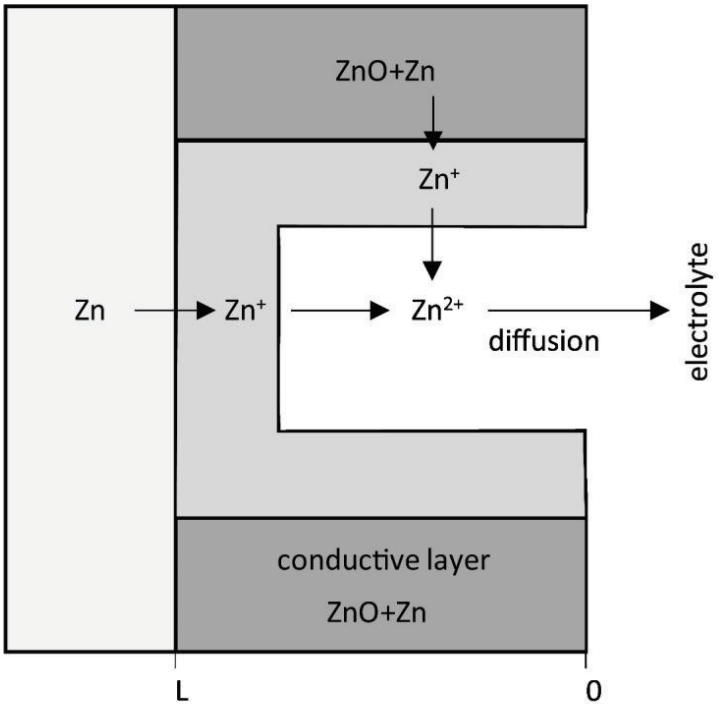

Fig. 26. Scheme of the stratified layer interphase (after Cachet et al. [121]).

collapse. Macdonald et al. [95] described the criterion for the local breakdown as follows:

$$(J_{ca} - J_m)\cdot(t - \tau) \geq \xi \quad (23)$$

where J_{ca} is the cation diffusion rate in the film, which increases for decreasing $V_{\ddot{O}}$ concentration, J_m the rate of submergence of the metal cation vacancies into the bulk of metal, t is the time required for $V_M^{X'}$ to accumulate to a critical amount ξ and τ is a constant.

With understanding of the described electrode processes (XIX–XXII) the effect of electrolyte additives on the growth of passive films can also be explained. As discussed in Chap. 5.2, some salts as additives had a positive effect on the passivation time of zinc. Macdonald et al. [95] explained this phenomenon for the case of chloride ions. They assumed that Cl^- ions were able to occupy the oxygen vacancies in the film and prevent the passive film growth. Furthermore, chloride ions support the active dissolution of the metal by affecting the cation diffusion rate. The authors demonstrated the ability of the model to describe dependencies of the time t (23) and the chloride concentration on the film breakdown overpotential in good accuracy with experimental results.

In further works, Macdonald et al. extended the point defect model for interpretation of the impedance response of passive films under dynamic conditions [134,135] and in order to explain the formation of bi-layer passive films [118,136,137]. In [27] the authors applied the model to zinc in alkaline electrolyte (pH 10.5). It is, however, important to mention that only the growth of the passive film type 2 was considered in this work. Macdonald reviewed the development of his complex point defect model several times [94,136]. It provides a logarithmic growth low of the passive layer on metals and was successfully validated in experimental samples with different anodes and conditions. The PDM gives furthermore a general physical explanation for the appearance, thickening and dissolution of the passive layer on metal electrodes.

Further research effort was placed on models for the analysis of impedance spectra. Based on earlier works of Park and Macdonald [138] and de Levie et al. [139], Cachet et al. [51,56,100,121–123] developed models for the cathodic deposition and the anodic dissolution on zinc electrodes. It is assumed that the active dissolution [51,56] of zinc occurs at a conductive, porous layer on the surface of the electrode. Since there is still disagreement about the exact mechanism of dissolution in the active and passive state [49,68,117], Cachet et al. proposed a simplified two-step discharge, the steps of which are $Zn \rightleftarrows Zn^+ + e^-$ and $Zn^+ \rightleftarrows Zn^{2+} + e^-$ (Fig. 26). Here, one can see the porous structure of the film on the surface of the electrode assumed to consist of cylindrical pores within a conductive material, which is a mixture of zinc and its oxides of the general composition Zn_xO_y. The inner layer of these pores is the reactive phase, where the active intermediate Zn^+ is present.

The two-step mechanism of charge transfer involves at least a monovalent intermediate formed in a thin reactive interphase separating the solid material from the electrolyte and whose conductivity is potential activated. The zincate ions formed at the pore bases partially precipitate inside the pores and mostly escape from the pores by a diffusion process the rate of which raises with decreasing pore length.

The model of charge transfer explains the following phenomena in complex impedance plots (Fig. 27):

i) The high frequency capacitive (HFC) loop, characterized by high values of capacity related to the current penetration within the pores.
ii) A high frequency inductive (HFI) loop corresponding to the intermediate Zn^+.

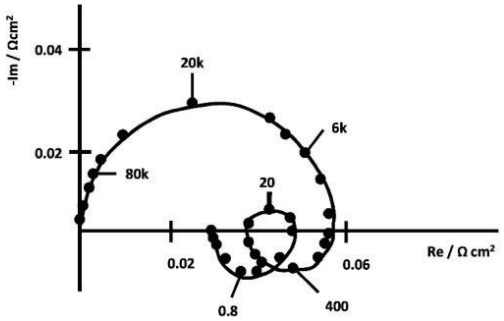

Fig. 27. Complex plane Nyquist plot (after Cachet et al. [121]), frequency given in Hz.

iii) A low frequency capacitive (LFC) loop resulting from the precipitation and diffusion process of Zn^{2+}.
iv) A low frequency inductive (LFI) loop resulting from the slow degradation with increasing anodic polarization.

This complex model for impedance measurements is able to describe the mechanism of zinc dissolution at the passivated electrode. The pore structure seems to be a well-chosen assumption for the given system to describe it mathematically. With the introduced model Cachet et al. were also able to show the influences of additives throughout the porous layer by assuming that these additives interfere with the interfacial reactions to generate a less conductive and geometrically different porous layer (cf. Chap. 5.2). An improvement could be e.g. to implement the porosity and tortuosity of the film to give an even more realistic description of the system.

7. Conclusions

The present review critically discusses the existing knowledge about the passivation process on zinc anodes in contact with alkaline electrolyte. Despite numerous investigations over several decades, no general consensus about the underlying mechanisms and the strategies to prevent passivation, which eventually leads to breakdown of the electrode activity, could be achieved. It is interesting to note that in many investigations either the dissolution-precipitation or the solid state passivation mechanism was assumed to proceed. A closer look reveals that the dissolution-precipitation theory was mainly used for interpretation of galvanostatic measurements while the solid state mechanism was preferred in case of potentiodynamic investigation. It is therefore necessary to conduct further systematic measurements in which both the potential and the concentration of zincates at the electrode surface can be precisely controlled. Thereby it would be possible to distinguish between conditions where a critical zincates concentration leads to precipitation of so-called type 1 films and the potential-driven direct oxidation of the zinc surface, which leads to formation of type 2 passive films. For these measurements it is recommended to use a combination of electrochemical and spectroscopic techniques.

It should be also mentioned that several investigations in literature dealing with the onset of passivation were carried out at conditions not relevant for battery applications. In a battery it is not possible to drive the zinc electrode to positive potentials, because even in the case of a short circuit the maximum potential of zinc is 0 V. For battery applications it would be more important to detect the starting point of film formation in order to prevent an activity loss of the electrode. Previous studies on the influence of

convection, temperature and electrolyte composition (including additives) already show important tendencies. It could be shown that the insufficient rate of hydroxide ions diffusion was the cause for the formation of the passive film by precipitation of an oxide layer, which could be prevented by forced convection. The conductivity of the alkaline electrolyte has a direct influence on the critical current density for anodic zinc dissolution. The ideal concentration of potassium hydroxide solution was found to be in the range of 7 mol/L. Zincate ions decrease the conductivity of the electrolyte remarkably. In contrary, some salts such as NaCl or Na_2SO_3 as additives showed a positive effect of the dissolution time of a zinc anode. However, a well-founded quantitative description of the influence of these parameters on the growth of passive films still needs to be made.

Another aspect not mentioned in most publications on zinc passivation is the quality of the zinc used. It can be expected that the passivation behavior is different depending on whether the investigated zinc is a polished plate, made by a calendering rolling process, or electrochemically deposited. A mechanical treatment of zinc, e.g. through a rolling process, influences the microcrystalline structure of the metal, which might have an effect on the dissolution behavior. This is well known from corrosion investigations, where it was shown that a previously bended metal has a higher corrosion rate than a mechanically untreated metal [140]. This may be one of the reasons why the investigation of passivation effects leads to contradictory results.

The description of the passivation process by mathematical models ranges from simple approaches like the Sand equation to complex modeling that is only feasible with the processing power of the computers used today. Our analysis of the existing literature revealed that the majority of the models are zero dimensional and aiming at calculation of the passivation time. Although the Sand equation was developed for systems in the absence of convective mass transport it could be later shown that application to conditions with stirred or flowing electrolyte is possible. However, the obtained model parameters must be treated with caution and cannot be transferred directly to other conditions.

The behavior of the electrode during passivation and in the passive state was also successfully modeled. Most of these models are based on the "dissolution-precipitation" mechanism and describe the formation of zinc oxide or hydroxide films. For the kinetics of zinc dissolution and deposition a two-step mechanism allows a good description of the experimental data. However, these models consider only the formation of type 1 passive films and disregard the potential-driven direct oxidation of the zinc surface. The most detailed and complex mathematical model for the passivation of metals has been developed by Macdonald. In contrast to other models, it considers the appearance of type 2 passive film on different metals according to the "nucleation and growth" model and enables the interpretation of its thickening and possible breakdown. Furthermore, the point defect model provides a physical explanation of the effects of different experimental conditions like the electrolyte composition or the applied potential on the structure and growth kinetics of the passive layer. On the other hand, the PDM does not consider the formation of type 1 passive films and has probably therefore not yet achieved more widespread attention among other groups active in the field of zinc passivation. In summary, it can be stated that there is no general model available at present that quantitatively describes the formation of different types of passive films on zinc depending on the operational conditions.

Acknowledgements

Part of this work was supported by the German Federal Ministry for Economic Affairs and Energy during the ZnPLUS project (grant number 03ESP217 E). The authors also thank two anonymous reviewers for critically reading the manuscript and suggesting substantial improvements.

References

[1] K. Harting, U. Kunz, T. Turek, Zinc-air batteries: Prospects and challenges for future improvement, Z. Phys. Chem 226 (2012) 151.
[2] G.X. Zhang, A dual power cell for storing electricity in zinc metal, J. Power Sources 285 (2015) 580–587.
[3] C. Gandenberger, F. Marscheider-Weidemann, L. Tercero, Kritische Rohstoffe aus europäischer Sicht, Die Volkswirtschaft: Das Magazin für Wirtschaftspolitik 11 (2010) 12–15.
[4] D. Linden, T.B. Reddy, Handbook of Batteries, McGraw-Hill, New York, 2001.
[5] W.-B. Cai, Q. Shi, M.F. Mansuetto, D.A. Scherson, In situ Raman spectroscopy on an operating AA Zn-MnO_2 battery under high discharge currents, Electrochem. Solid-State Lett. 3 (2000) 319–320.
[6] S.S. Abd El Rehim, S.M. Abd El Wahab, E.E. Fouad, H.H. Hassan, Passivity and passivity breakdown of zinc anode in alkaline medium, Mater. Corros. 46 (1995) 633–638.
[7] A. Nakata, K. Fukuda, H. Murayama, H. Tanida, T. Yamane, H. Arai, Y. Uchimoto, K. Sakurai, Z. Ogumi, Operando X-ray fluorescence imaging for zinc-based secondary batteries, Electrochemistry 83 (2015) 849–851.
[8] P. Kurzweil, Brennstoffzellentechnik: Grundlagen Systeme, Komponenten Vieweg+Teubner Verlag Anwendungen, Wiesbaden, 2003.
[9] C.F. Schönbein, Bemerkungen über Faraday's Hypothese in Betreff der Ursache der Passivität des Eisens in Salpetersäure, Ann. Phys. 115 (1836) 137–141.
[10] W. Hisinger, J. Berzelius, Galvanisch – electrische Untersuchungen, Ann. Phys. 27 (1807) 269–324.
[11] Martens, Über die Passivität des Eisens, veranlasst durch einen Aufsatz des Hrn. Schönbein, Ann. Phys. 137 (1844) 121–129.
[12] W.J. Müller, Zur Theorie der Passivitätserscheinungen, Über den Stromdurchgang durch Anoden, welche mit einer nicht löslichen Deckschicht bedeckt sind, Monatsh. Chem. 12 (1930) 191–196.
[13] W.J. Müller, On the passivity of metals, T. Faraday Soc. 27 (1931) 737–751.
[14] K. Huber, Studien zur Chemie und zur Struktur anodisch erzeugter Niederschläge und Deckschichten. I. Mitteilung. Über das anodische Verhalten von Zink in Natronlauge als Badflüssigkeit, Helv. Chim. Acta 26 (1943) 1037–1054.
[15] K.J. Vetter, Elektrochemische Kinetik, Springer-Verlag, Berlin-Göttingen-Heidelberg, 1961.
[16] K.J. Vetter, Über den Mechanismus der elektrolytischen Passivschichtbildung, in: H. Fischer, K. Hauffe, W. Wiederholt (Eds.), Passivierende Filme und Deckschichten, Springer-Verlag, Berlin Heidelberg, 1956, pp. 72–91.
[17] K. Huber, Anodic formation of coatings on magnesium, zinc, and cadmium, J. Electrochem. Soc. 100 (1953) 376–382.
[18] R. Landsberg, Zum anodischen Verhalten des Zinks in Natronlauge, Z. Phys. Chem. 206 (1957) 289–291.
[19] R. Landsberg, H. Bartelt, Bedeckungsvorgänge an Zinkanoden in Natronlauge, Z. Elektrochem. 61 (1957) 1161–1168.
[20] X.G. Zhang, Corrosion and electrochemistry of zinc, Plenum Press, New York, 1996.
[21] M.B. Liu, G.M. Cook, N.P. Yao, in: N.T.I. Service (Ed.), Galvanostatic polarization of zinc microanodes in KOH electrolytes, Argonne National Library, Argone, Illinois, 1980.
[22] R.D. Armstrong, M.F. Bell, The electrochemical behaviour of zinc in alkaline solution, in: H.R. Thirsk (Ed.), Electrochemistry, vol. 4, The Chemical Society, London, 1974.
[23] C.G. Smith, Ellipsometry of anodic film growth, U.S. Departmend of Energy University of California, Berkeley California, 1978.
[24] J.R. Vilche, K. Jüttner, W.J. Lorenz, W. Kautek, W. Paatsch, M.H. Dean, U. Stimming, Semiconductor properties of passive films on Zn, Zn-Co, and Zn-Ni substrates, J. Electrochem. Soc. 136 (1989) 3773–3779.
[25] A.L. Rudd, C.B. Breslin, Photo-induced dissolution of zinc in alkaline solutions, Electrochim. Acta 45 (2000) 1571–1579.
[26] A. Fattah-alhosseini, M. Mirshekari, Effect of film formation potential on the electrochemical behavior of the passive films formed on zinc in 0.01 M NaOH, T. Indian I. Metals. 68 (2015) 851–857.
[27] D.D. Macdonald, K.M. Ismail, E. Sikora, Characterization of the passive state on zinc, J. Electrochem. Soc. 145 (1998) 3141–3149.
[28] J.C. Buchholz, Surface electronic structure for the initial stages of electrochemical oxidation of zinc, Surf. Sci. 101 (1980) 146–154.
[29] P. Scholl, X. Shan, D. Bonham, G.A. Prentice, Photoelectrochemical characterization of the anodic film on zinc in KOH solution, J. Electrochem. Soc. 138 (1991) 895–899.
[30] N.A. Hampson, M.J. Tarbox, J.T. Lilley, P.G. Farr, The passivation of vertical zinc anodes in potassium hydroxide solution, Electrochem. Technol. 2 (1964) 309–313.
[31] S. Thomas, N. Birbilis, M.S. Venkatraman, I.S. Cole, Corrosion of zinc as a function of pH, Corros. Sci. 68 (2012).
[32] S. Thomas, I.S. Cole, M. Sridhar, N. Birbilis, Revisiting zinc passivation in alkaline solutions, Electrochim. Acta 97 (2013) 192–201.

[33] Z.I. Nikitina, Passivation of zinc electrodes in galvanic cells with alkaline electrolytes, J. Appl. Chem. USSR 31 (1958) 209–216.
[34] J. Euler, Zur Langzeitpassivierung von Zink in Zinkat-haltiger Kalium-Hydroxid-Lösung, Electrochim. Acta 11 (1966) 701–715.
[35] W.R. Dunstan, H.A. Dickinson, J. Goulding, E. Goulding, The rusting of iron, J. Chem. Soc. Trans. 87 (1905) 1548–1574.
[36] J.R. Churchill, The formation of hydrogen peroxide during corrosion reactions, ECS Trans. 76 (1939) 341–357.
[37] M.N. Hull, J.E. Ellison, J.E. Toni, The anodic behaviour of zinc electrodes in potassium hydroxide electrolytes, J. Electrochem. Soc. (1970).
[38] H. Fry, M. Whitaker, The anodic oxidation of zinc and a method of altering the characteristics of the anodic films, J. Electrochem. Soc. 106 (1959) 606–611.
[39] T.P. Dirkse, Electrolytic Oxidation of Zinc in Alkaline Solutions, J. Electrochem. Soc. 102 (1955) 497–501.
[40] R.W. Powers, M.W. Breiter, The anodic dissolution and passivation of zinc in concentrated potassium hydroxide solutions, J. Electrochem. Soc. 116 (1969) 719–728.
[41] M.C. Bernard, A. Hugot-Le Goff, N. Phillips, In situ Raman study of the corrosion of zinc-coated steel in the presence of chloride: II. Mechanisms of underpaint corrosion and role of the conversion layers, J. Electrochem. Soc. 142 (1995) 2167–2170.
[42] A. Hugot-Le Goff, S. Joiret, B. Saïdani, R. Wiart, In-situ Raman spectroscopy applied to the study of the deposition and passivation of zinc in alkaline electrolytes, J. Electroanal. Chem. 263 (1989) 127–135.
[43] Q. Shi, L.J. Rendek, W.-B. Cai, D.A. Scherson, In situ Raman spectroscopy of single particle microelectrodes: zinc passivation in alkaline electrolytes, Electrochem. Solid-State Lett. 6 (2003) E35–E39.
[44] M.C. Bernard, A. Hugot-Le Goff, N. Phillips, In situ Raman study of the corrosion of zinc-coated steel in the presence of chloride: I. Characterization and stability of zinc corrosion products, J. Electrochem. Soc. 142 (1995) 2162–2167.
[45] M. Mokaddem, P. Volovitch, K. Ogle, The anodic dissolution of zinc and zinc alloys in alkaline solution. I. Oxide formation on electrogalvanized steel, Electrochim. Acta 55 (2010) 7867–7875.
[46] R.D. Armstrong, G.M. Bulman, The anodic dissolution of zinc in alkaline solutions, J. Electroanal. Chem. 25 (1970) 121–130.
[47] P.G. Farr, N.A. Hampson, The exchange reaction Zn(II)/Zn(Hg) in alkali, J. Electroanal. Chem. 18 (1968) 407–411.
[48] J.P.G. Farr, N.A. Hampson, Reactions at solid metal electrodes. Part 1.-Faradaic impedance of zinc electrodes in alkaline solution, T. Faraday Soc. 62 (1966) 3493–3501.
[49] J.O.M. Bockris, Z. Nagy, A. Damjanovic, On the deposition and dissolution of zinc in alkaline solutions, J. Electrochem. Soc. 119 (1972) 285–295.
[50] B.D. Cahan, Z. Nagy, M.A. Genshaw, Cell design for potentiostatic measuring system, J. Electrochem. Soc. 119 (1972) 64–69.
[51] C. Cachet, B. Saidani, R. Wiart, The behaviour of zinc electrode in alakaline electrolyte I. A kinetic analysis of cathodic deposition, J. Electrochem. Soc. 138 (1992) 678–687.
[52] N.A. Hampson, G.A. Herdman, R. Taylor, Some kinetic and thermodynamic studies of the system Zn/Zn(II), OH^-, J. Electroanal. Chem. Interfacial Electrochem. 25 (1970) 9–18.
[53] T.P. Dirkse, N.A. Hampson, The anodic behaviour of zinc in aqueous KOH solution—I. Passivation experiments at very high current densities, Electrochim. Acta 16 (1971) 2049–2056.
[54] S.K. Sharma, M.D. Reed, Raman study of zincate ions in concentrated alkaline solutions, J. Inorg. Nucl. Chem. 38 (1976) 1971–1972.
[55] Y.C. Chang, G. Prentice, A model for the anodic dissolution of zinc in alkaline electrolyte: Kinetics of initial dissolution, J. Electrochem. Soc. 131 (1984) 1465–1468.
[56] C. Cachet, B. Saidani, R. Wiart, The behaviour of zinc electrode in alkaline electrolytes II. A kinetic analysis of anodic dissolution, J. Electrochem. Soc. 139 (1992) 645–654.
[57] A.J. Bard, Encyclopedia of electrochemistry of the elements, Marcel Dekker INC., New York Basel, 1976.
[58] R.D. Armstrong, Diagnostic criteria for distinguishing between the dissolution-precipitation and the solid state mechanisms of passivation, Corros. Sci. 11 (1971) 693–697.
[59] P.L. Cabot, M. Cortes, C.F.F. Perez, Potentiostatic passivation of zinc in alkaline solutions, J. Appl. Electrochem. 23 (1992) 371–378.
[60] C.J. Bushrod, N.A. Hampson, The anodic behaviour of zinc in KOH solution. V: Galvanostatic polarization with an interruption, J. Appl. Electrochem. 1 (1971) 99–101.
[61] S. Szpak, C.J. Gabriel, The Zn-KOH system: The solution-precipitation path for anodic ZnO formation, J. Electrochem. Soc. 126 (1979) 1914–1923.
[62] M.B. Liu, G.M. Cook, N.P. Yao, Passivation of zinc anodes in KOH electrolytes, J. Electrochem. Soc. 128 (1981) 1663–1668.
[63] N.A. Hampson, P.E. Shaw, R. Taylor, Anodic behaviour of zinc in potassium hydroxide solution, Br. Corros. J. 4 (1969).
[64] T.P. Dirkse, The behavior of the zinc electrodes in alkaline solutions, J. Electrochem. Soc. 128 (1981) 1412–1415.
[65] T.P. Dirkse, D.J. Kroon, Effect of ionic strengt in the passivation of ionic zinc electrodes in KOH solutions, J. Appl. Electrochem. 1 (1971).
[66] T.P. Dirkse, N.A. Hampson, The anodic behaviour of zinc in aqueous solution—III. Passivation in mixed KF-KOH solutions, Electrochim. Acta 17 (1972) 813–818.
[67] I. Sanghi, M. Fleischmann, Some potentiostatic studies on zinc, Electrochim. Acta 1 (1959) 161–176.
[68] T.P. Dirkse, N.A. Hampson, The anodic behaviour of zinc in aqueous KOH solution—II. Passivation experiments using linear sweep voltammetry, Electrochim. Acta 17 (1972) 387–394.
[69] R.D. Armstrong, G.M. Bulman, H.R. Thirsk, The passivation of zinc amalgam in alkaline solutions, J. Electroanal. Chem. 22 (1969) 55–62.
[70] H. Kaesche, The passivity of zinc in aqueous solutions of sodium carbonate and sodium bicarbonate, Electrochim. Acta 9 (1964) 383–394.
[71] B. Kabanov, R. Burstein, A. Frumkin, Kinetics of electrode processes on the iron electrode, Discuss. Faraday Soc. 1 (1947) 259–269.
[72] A.I. Oshe, Y.Y. Kulyavik, T.I. Popova, B.N. Kabanov, Use of rotating disc electrode with ring to study the mechanism of the passivation of metals, Sov. Electrochem. 2 (1966) 1356–1357.
[73] B. Kabanov, La theorie de la passivation du zinc et la possibilite de la transition des couches d'adsorption passivantes en couches epaisses, Electrochim. Acta 6 (1962) 253–257.
[74] L.M. Baugh, A. Higginson, Passivation of zinc in concentrated alkaline solution—I. Characteristics of active dissolution prior to passivation, Electrochim. Acta 30 (1985) 1163–1172.
[75] N.A. Hampson, M.J. Tarbox, The anodic behavior of zinc in potassium hydroxide solution, J. Electrochem. Soc (1963) 95–98.
[76] M. Eisenberg, H.F. Bauman, D.M. Brettner, Gravity field effects on zinc anode discharge in alkaline media, J. Electrochem. Soc. 108 (1961) 909–915.
[77] J.P. Elder, The electrochemical behavior of zinc in alkaline media, J. Electrochem. Soc. 116 (1969) 757–762.
[78] R.N. Elsdale, N.A. Hampson, P.C. Jones, A.N. Strachan, The anodic behaviour of porous zinc electrodes, J. Appl. Electrochem. 1 (1971) 213–217.
[79] T.I. Popova, N.A. Simonova, B.N. Kabanov, Mechanism of passivation of zinc in strong zincate solutions of alkali, Sov. Electrochem. 2 (1966) 1347–1350.
[80] L.M. Baugh, A.R. Baikie, Passivation of zinc in concentrated alkaline solution—II. Role of various experimental factors and the distinction between the solid-state and dissolution—precipitation mechanisms, Electrochim. Acta 30 (1985) 1173–1183.
[81] M. Cai, S.M. Park, Oxidation of zinc in alkaline solutions studied by electrochemical impedance spectroscopy, J. Electrochem. Soc. 143 (1996) 3895–3902.
[82] I. Sanghi, W.F.K. Wynne-Jones, Electrochemical behaviour of zinc in alkaline solutions, P. Indian Acad. Sci. A 47 (1958) 49–64.
[83] H.J.S. Sand, On the concentration at the electrodes in a solution, with special reference to the liberation of hydrogen by electrolysis of a mixture of copper sulphate and sulphuric acid, Philos, Mag. Series 6 (1) (1901) 45–79.
[84] P. Delahay, C.C. Mattax, T. Berzins, Theory of voltammetry at constant current. IV. Electron transfer followed by chemical reaction, J. Am. Chem. Soc. 76 (1954) 5319–5324.
[85] M.J. Brook, N.A. Hampson, The anodic behaviour of zinc in KOH solution—IV. Anodic experiments in flowing electrolyte, Electrochim. Acta 15 (1970) 1749–1758.
[86] A. Marshall, N.A. Hampson, The point of passivation of a zinc electrode in alkali, J. Appl. Electrochem. 7 (1977) 271–273.
[87] M.C.H. McKubre, D.D. Macdonald, The dissolution and passivation of zinc in concentrated aqueous hydroxide, J. Electrochem. Soc. 128 (1981) 524–530.
[88] S.C. Barton, A.C. West, Electrodissolution of zinc at the limiting current, J. Electrochem. Soc. 148 (2001) A490–A495.
[89] Y. Ko, S.-M. Park, Zinc oxidation in dilute alkaline solutions studied by real-time electrochemical impedance spectroscopy, J. Phys. Chem. C 116 (2012) 7260–7268.
[90] M.N. Hull, J.E. Toni, Formation and reduction of films on amalgamated and non-amalgamated zinc electrodes in alkaline solutions, T. Faraday Soc. 67 (1971) 1128–1136.
[91] V.G. Levich, Physicochemical hydrodynamics, State publisher of physicomathematical literature, Moscow, 1959.
[92] T.I. Popova, G.L. Vidovich, N.A. Simonova, B.N. Kabanov, Anodic dissolution of deeply passivated zinc in alkaline solution supersaturated with zincate, Sov. Electrochem. 3 (1967) 860–862.
[93] T.I. Popova, N.A. Simonova, K.B.N, Anodic dissolution of passive zinc in zincate solutions of alkali, Sov. Electrochem. 3 (1967) 1273–1279.
[94] D.D. Macdonald, The history of the point defect model for the passive state: A brief review of film growth aspects, Electrochim. Acta 56 (2011) 1761–1772.
[95] L.F. Lin, C.Y. Chao, D.D. Macdonald, A point defect model for anodic passive films: II. Chemical breakdown and pit initiation, J. Electrochem. Soc. 128 (1981) 1194–1198.
[96] C.Y. Chao, L.F. Lin, D.D. Macdonald, A point defect model for anodic passive films: I. Film growth kinetics, J. Electrochem. Soc. 128 (1981) 1181–1187.
[97] R.W. Powers, An electrochemical cell for microscopic observation of an electrode under polarization, Electrochem. Tech. (1967).
[98] L. Sziráki, Á. Cziráki, I. Gerőcs, Z. Vértesy, L. Kiss, A kinetic model of the spontaneous passivation and corrosion of zinc in near neutral Na_2SO_4 solutions, Electrochim. Acta 43 (1998) 175–186.
[99] B. Aurian-Blajeni, M. Tomkiewicz, The passivation of zinc in alkaline solutions, J. Electrochem. Soc. 132 (1985) 1511–1515.
[100] C. Cachet, U. Ströder, R. Wiart, The kinetics of zinc electrode in alkaline zincate electrolytes, Electrochim. Acta 27 (1982) 903–908.
[101] S. Bhadra, A.G. Hsieh, M.J. Wang, B.J. Hertzberg, D.A. Steingart, Anode characterization in zinc-manganese dioxide AA alkaline batteries using

electrochemical-acoustic time-of-flight analysis, J. Electrochem. Soc. 163 (2016) A1050–A1056.
[102] I. Arise, S. Kawai, Y. Fukunaka, F.R. McLarnon, Coupling phenomena between zinc surface morphological variations and ionic mass transfer rate in alkaline solution, J. Electrochem. Soc. 160 (2013) D66–D74.
[103] A.G. Briggs, N.A. Hampson, A. Marshall, Concentrated potassium zincate solutions studied using laser Raman spectroscopy and potentiometry, Journal of the Chemical Society, Faraday Transactions 2 (70) (1974) 1978–1990.
[104] Y. Chen, A. Erbe, In situ spectroscopic ellipsometry during electrochemical treatment of zinc in alkaline carbonate electrolyte, Surf. Sci. 607 (2013) 39–46.
[105] C. Mele, B. Bozzini, Spectroelectrochemical investigation of the anodic and cathodic behaviour of zinc in 5.3 M KOH, J. Appl. Electrochem. 45 (2015) 43–50.
[106] X. Shan, D. Ren, P. Scholl, G. Prentice, Coulometric and ellipsometric measurements of passive film thickness on zinc electrodes in KOH solution, J. Electrochem. Soc. 136 (1989) 3594–3598.
[107] R.J. Gilliam, J.W. Graydon, D.W. Kirk, S.J. Thorpe, A review of specific conductivities of potassium hydroxide solutions for various concentrations and temperatures, Int. J. Hydrogen Energy 32 (2007) 359–364.
[108] D.M. See, R.E. White, Temperature and concentration dependence of the specific conductivity of concentrated solutions of potassium hydroxide, J. Chem. Eng. Data 42 (1997) 1266–1268.
[109] A. Marshall, N.A. Hampson, J.S. Drury, The discharge behaviour of the zinc/air slurry cell, I. Electroanal. Chem. Interfacial Electrochem. 59 (1975) 33–40.
[110] L. Vanyukova, B. Kabanov, Tranlated from Russian: Activation of iron with clorine during anodic polarisation, Dokl. Akad. Nauk SSSR 59 (1948) 917–920.
[111] H. Yang, Y. Cao, X. Ai, L. Xiao, Improved discharge capacity and suppressed surface passivation of zinc anode in dilute alkaline solution using surfactant additives, J. Power Sources 128 (2004) 97–101.
[112] A.R. Mainar, O. Leonet, M. Bengoechea, I. Boyano, I. de Meatza, A. Kvasha, A. Guerfi, J. Alberto Blázquez, Alkaline aqueous electrolytes for secondary zinc–air batteries: an overview, Int. J. Energy Res. (2016).
[113] M. Minakshi, D. Appadoo, D.E. Martin, The anodic behavior of planar and porous zinc electrodes in alkaline electrolyte, Electrochem. Solid-State Lett. 13 (2010) A77–A80.
[114] E. Deiss, F. Holzer, O. Haas, Modeling of an electrically rechargeable alkaline Zn–air battery, Electrochim. Acta 47 (2002) 3995–4010.
[115] D. Schröder, U. Krewer, Model based quantification of air-composition impact on secondary zinc air batteries, Electrochim. Acta 117 (2014) 541–553.
[116] E.D. Farmer, A.H. Webb, Zinc passivation and the effect of mass transfer in flowing electrolyte, J. Appl. Electrochem. 2 (1972) 123–136.
[117] A.R. Despić, D. Jovanović, T. Rakić, Kinetics and mechanism of deposition of zinc from zincate in concentrated alkali hydroxide solutions, Electrochim. Acta 21 (1976) 63–77.
[118] D.D. Macdonald, G. Englehardt, The point defect model for bi-layer passive films, ECS Trans. 28 (2010) 123–144.
[119] W.G. Sunu, D.N. Bennion, Transient and failure analyses of the porous zinc electrode, J. Electrochem. Sci. Technol. 127 (1980) 2007–2016.
[120] P.L. Cabot, M. Cortés, F.A. Centellas, J.A. Garrido, E. Pérez, Potentiodynamic passivation of zinc in aqueous KOH solutions, J. Electroanal. Chem. 201 (1986) 85–100.
[121] C. Cachet, B. Saïdani, R. Wiart, The kinetics of zinc deposition at low overpotentials in alkaline electrolytes, Electrochim. Acta 33 (1988) 405–416.
[122] C. Cachet, B. Saïdani, R. Wiart, A model for zinc deposition in alkaline electrolytes: Inhibition layer and activation mechanism, Electrochim. Acta 34 (1989) 1249–1250.
[123] C. Cachet, R. Wiart, J. Zoppas-Ferreira, Zinc deposition and dissolution in a flow-through porous electrode, Electrochim. Acta 38 (1993) 311–318.
[124] M.J. Isaacson, F.R. McLarnon, E.J. Cairns, Current density and ZnO precipitation-dissolution distributions in Zn - ZnO porous electrodes and their effect on material redistribution: A two-dimensional mathematical model, J. Electrochem. Soc. 137 (1990) 2014–2021.
[125] Z. Mao, R.E. White, Mathematical modeling of a primary zinc/air battery, J. Electrochem. Soc. 139 (1992).
[126] I. Arise, S. Kawai, Y. Fukunaka, F.R. McLarnon, Numerical calculation of ionic mass-transfer rates accompanying anodic zinc dissolution in alkaline solution, J. Electrochem. Soc. 157 (2010) A171–A178.
[127] H. Song, X. Xu, L. Fen, Numerical simulation of discharge process and failure mechanisms of zinc electrode, Acta Phys.-Chim. Sin. 29 (2013) 1961–1974.
[128] I.G. Bosco, I.S. Cole, B. Emmanuel, Regulation of interfacial chemistry by coupled reaction-diffusion processes in the electrolyte: A stiff solution dynamics model for corrosion and passivity of metals, J. Electroanal. Chem. 722–723 (2014) 68–77.
[129] H.F. Weber, Untersuchungen über das Elementargesetz der Hydrodiffusion, Ann. Phys. 243 (1879) 536–552.
[130] W. Müller, Zur Theorie der Passivitätserscheinungen I–XXXI, Monatsh. Chem. (1928-1937) 60–70.
[131] A.J. Calandra, N.R. deTacconi, R. Pereiro, A.J. Arvia, Potentiodynamic current/potential relations for film formation under ohmic resistance control, Electrochim. Acta 19 (1974) 901–905.
[132] A.G. Briggs, N.A. Hampson, A. Marshall, Concentrated potassium zincate solutions studied using laser Raman spectroscopy and potentiometry. J. Chem. Soc, Faraday Trans. 70 (1974) 1978–1990.
[133] D.D. Macdonald, M. Urquidi-Macdonald, Theory of steady-state passive films, J. Electrochem. Soc. 137 (1990) 2395–2402.
[134] D.D. Macdonald, E. Sikora, G. Engelhardt, Characterizing electrochemical systems in the frequency domain, Electrochim. Acta 43 (1998) 87–107.
[135] C.Y. Chao, L.F. Lin, D.D. Macdonald, A point defect model for anodic passive films: III. Impedance response, J. Electrochem. Soc. 129 (1982) 1874–1879.
[136] D.D. Macdonald, The point defect model for the passive state, J. Electrochem. Soc. 139 (1992) 3434–3449.
[137] L. Zhang, D.D. Macdonald, E. Sikora, J. Sikora, On the kinetics of growth of anodic oxide films, J. Electrochem. Soc. 145 (1998) 898–905.
[138] J.R. Park, D.D. Macdonald, Impedance studies of the growth of porous magnetite films on carbon steel in high temperature aqueous systems, Corros. Sci. 23 (1983) 295–315.
[139] R.D. Levie, P. Delahay (Eds.), Advances in electrochemistry and electrochemical engineering, 6, Wiley Interscience, New York, 1967, pp. 329.
[140] S. Lower, Electrochemical Corrosion, (2016) http://www.chem1.com/acad/webtext/elchem/ec7.html, 07-27-2016.